# The comparative osteology of *Plesiochelys bigleri* n. sp., a new coastal marine turtle from the Late Jurassic of Porrentruy (Switzerland) (#16722)

First submission

Please read the **Important notes** below, the **Review guidance** on page 2 and our **Standout reviewing tips** on page 3. When ready **submit online**. The manuscript starts on page 4.

### Important notes

### **Editor and deadline**

Mark Young / 30 Mar 2017

Files 19 Figure file(s)

5 Table file(s)

Please visit the overview page to **download and review** the files

not included in this review PDF.

**Describes a new species.** 



Please read in full before you begin

### How to review

When ready <u>submit your review online</u>. The review form is divided into 5 sections. Please consider these when composing your review:

- 1. BASIC REPORTING
- 2. EXPERIMENTAL DESIGN
- 3. VALIDITY OF THE FINDINGS
- 4. General comments
- 5. Confidential notes to the editor
- 1 You can also annotate this PDF and upload it as part of your review

To finish, enter your editorial recommendation (accept, revise or reject) and submit.

#### **BASIC REPORTING**

- Clear, unambiguous, professional English language used throughout.
- Intro & background to show context.
  Literature well referenced & relevant.
- Structure conforms to **PeerJ standards**, discipline norm, or improved for clarity.
- Figures are relevant, high quality, well labelled & described.
- Raw data supplied (see **PeerJ policy**).

#### **EXPERIMENTAL DESIGN**

- Original primary research within **Scope of** the journal.
- Research question well defined, relevant & meaningful. It is stated how the research fills an identified knowledge gap.
- Rigorous investigation performed to a high technical & ethical standard.
- Methods described with sufficient detail & information to replicate.

### **VALIDITY OF THE FINDINGS**

- Impact and novelty not assessed.
  Negative/inconclusive results accepted.
  Meaningful replication encouraged where rationale & benefit to literature is clearly stated.
- Data is robust, statistically sound, & controlled.
- Conclusions are well stated, linked to original research question & limited to supporting results.
- Speculation is welcome, but should be identified as such.

The above is the editorial criteria summary. To view in full visit <a href="https://peerj.com/about/editorial-criteria/">https://peerj.com/about/editorial-criteria/</a>

### 7 Standout reviewing tips



The best reviewers use these techniques

|  | n |
|--|---|
|  | N |

## Support criticisms with evidence from the text or from other sources

### Give specific suggestions on how to improve the manuscript

### Comment on language and grammar issues

### Organize by importance of the issues, and number your points

### Give specific suggestions on how to improve the manuscript

## Please provide constructive criticism, and avoid personal opinions

# Comment on strengths (as well as weaknesses) of the manuscript

### **Example**

Smith et al (J of Methodology, 2005, V3, pp 123) have shown that the analysis you use in Lines 241-250 is not the most appropriate for this situation. Please explain why you used this method.

Your introduction needs more detail. I suggest that you improve the description at lines 57-86 to provide more justification for your study (specifically, you should expand upon the knowledge gap being filled).

The English language should be improved to ensure that your international audience can clearly understand your text. I suggest that you have a native English speaking colleague review your manuscript. Some examples where the language could be improved include lines 23, 77, 121, 128 - the current phrasing makes comprehension difficult.

- 1. Your most important issue
- 2. The next most important item
- 3. ...
- 4. The least important points

Line 56: Note that experimental data on sprawling animals needs to be updated. Line 66: Please consider exchanging "modern" with "cursorial".

I thank you for providing the raw data, however your supplemental files need more descriptive metadata identifiers to be useful to future readers. Although your results are compelling, the data analysis should be improved in the following ways: AA, BB, CC

I commend the authors for their extensive data set, compiled over many years of detailed fieldwork. In addition, the manuscript is clearly written in professional, unambiguous language. If there is a weakness, it is in the statistical analysis (as I have noted above) which should be improved upon before Acceptance.



# The comparative osteology of *Plesiochelys bigleri* n. sp., a new coastal marine turtle from the Late Jurassic of Porrentruy (Switzerland)

Christian Püntener  $^{\text{Corresp.},-1}$  , Jérémy Anquetin  $^{2,3}$  , Jean-Paul Billon-Bruyat  $^{1}$ 

Corresponding Author: Christian Püntener Email address: christian.puntener@jura.ch

**Background.** During the Late Jurassic several groups of eucryptodiran turtles inhabited the shallow epicontinental seas of Western Europe. Plesiochelyidae are an important part of this first radiation of crown group turtles into marine ecosystems. Fossils of Plesiochelyidae occur in many European localities, and are especially abundant in the Kimmeridgian layers of the Swiss Jura Mountains (Solothurn and Porrentruy). In the mid 19th century, the quarries of Solothurn (NW Switzerland) already provided a large amount of fossil turtles, most notably *Plesiochelys etalloni*, the best-known plesiochelyid species. Recent excavations in the Porrentruy area (NW Switzerland) revealed new fossils of *Plesiochelys*, including numerous well-preserved shells with associated cranial and postcranial material.

**Methods/Results.** Out of 80 shells referred to *Plesiochelys*, 41 are assigned to a new species, *Pl. bigleri* n. sp., including a skull-shell association. We furthermore refer 15 shells to *Pl. etalloni*, and 24 shells to *Plesiochelys* sp. Anatomical comparisons show that *Pl. bigleri* can clearly be differentiated from *Pl. etalloni* by cranial features. The shell anatomy and the appendicular skeleton of *Pl. bigleri* and *Pl. etalloni* are very similar. However, a statistical analysis demonstrates that the thickness of neural bones allows to separate the two species based on incomplete material. This study furthermore illustrates the extent of intraspecific variation in the shell anatomy of *Pl. bigleri* and *Pl. etalloni*. Our results represent an important point of comparison for future studies on Mesozoic turtle diversity.

<sup>1</sup> Section d'archéologie et paléontologie, Office de la culture, République et Canton du Jura, Porrentruy, Switzerland

<sup>&</sup>lt;sup>2</sup> JURASSICA Museum, Porrentruy, Switzerland

<sup>&</sup>lt;sup>3</sup> Department of Geosciences, University of Fribourg, Fribourg, Switzerland



| 1  | The comparative osteology of <i>Plesiochelys bigleri</i> n. sp., a new coastal marine turtle from        |
|----|--|
| 2  | the Late Jurassic of Porrentruy (Switzerland)  |
| 3  |  |
| 4  | Christian Püntener <sup>1</sup> , Jérémy Anquetin <sup>2, 3</sup> , Jean-Paul Billon-Bruyat <sup>1</sup> |
| 5  |  |
| 6  | <sup>1</sup> Section d'archéologie et paléontologie, Office de la culture, République et Canton du Jura, |
| 7  | Porrentruy, Switzerland  |
| 8  | <sup>2</sup> JURASSICA Museum, Porrentruy, Switzerland   |
| 9  | <sup>3</sup> Department of Geosciences, University of Fribourg, Fribourg, Switzerland                    |
| 10 |  |
| 11 | Corresponding Author:  |
| 12 | Christian Püntener   |
| 13 |  |
| 14 | Email address: christian.puntener@jura.ch  |
|    |  |



### 15 **ABSTRACT**

| 16 | Background. During the Late Jurassic several groups of eucryptodiran turtles innabited the                       |
|----|--|
| 17 | shallow epicontinental seas of Western Europe. Plesiochelyidae are an important part of this first               |
| 18 | radiation of crown group turtles into marine ecosystems. Fossils of Plesiochelyidae occur in                     |
| 19 | many European localities, and are especially abundant in the Kimmeridgian layers of the Swiss                    |
| 20 | Jura Mountains (Solothurn and Porrentruy). In the mid 19th century, the quarries of Solothurn                    |
| 21 | (NW Switzerland) already provided a large amount of fossil turtles, most notably <i>Plesiochelys</i>             |
| 22 | etalloni, the best-known plesiochelyid species. Recent excavations in the Porrentruy area (NW                    |
| 23 | Switzerland) revealed new fossils of <i>Plesiochelys</i> , including numerous well-preserved shells              |
| 24 | with associated cranial and postcranial material.  |
| 25 | Methods/Results. Out of 80 shells referred to <i>Plesiochelys</i> , 41 are assigned to a new species, <i>Pl.</i> |
| 26 | bigleri n. sp., including a skull-shell association. We furthermore refer 15 shells to Pl. etalloni,             |
| 27 | and 24 shells to <i>Plesiochelys</i> sp. Anatomical comparisons show that <i>Pl. bigleri</i> can clearly be      |
| 28 | differentiated from Pl. etalloni by cranial features. The shell anatomy and the appendicular                     |
| 29 | skeleton of Pl. bigleri and Pl. etalloni are very similar. However, a statistical analysis                       |
| 30 | demonstrates that the thickness of neural bones allows to separate the two species based on                      |
| 31 | incomplete material. This study furthermore illustrates the extent of intraspecific variation in the             |
| 32 | shell anatomy of Pl. bigleri and Pl. etalloni. Our results represent an important point of                       |
| 33 | comparison for future studies on Mesozoic turtle diversity.  |



### INTRODUCTION

- 35 The first radiation of crown-group turtles into marine environments occurred in Western Europe
- during the Late Jurassic. At that time, several groups of basal pan-cryptodiran turtles,
- traditionally referred to the families Plesiochelyidae Baur, 1888, Thalassemydidae Zittel, 1889,
- and Eurysternidae Dollo, 1886, colonized coastal ecosystems from restricted lagoons to more
- 39 open seaways. These turtles eventually disappeared at the Jurassic-Cretaceous boundary
- 40 following major sea-level changes that restricted their habitats (e.g., Bardet, 1994; Bardet, 1995;
- 41 Bardet et al., (2).
- Plesiochelyids are relatively large coastal marine turtles known from the Late Jurassic of
- 43 Switzerland, France, Germany, England, Spain, and Portugal. They are notably characterized by
- a fully ossified carapace and a series of derived basicranial features (Gaffney, 1975a; Gaffney,
- 45 1976; Anguetin, Püntener & Billon-Bruyat, 2015). *Plesiochelys etalloni* (Pictet & Humbert,
- 46 1857) is undoubtedly the best known plesiochelyid turtle, thanks notably to numerous specimens
- found in Solothurn, Switzerland (Rütimeyer, 1873; Bräm, 1965; Gaffney, 1975a; Gaffney, 1976;
- 48 Anquetin, Püntener & Billon-Bruyat, 2014; Anquetin, Püntener & Billon-Bruyat, 2015).
- 49 Plesiochelys etalloni is known by both skulls and shells from the Kimmeridgian of the Swiss and
- 50 French Jura Mountains, southern England, and northwestern Germany (Pictet & Humbert, 1857;
- Rütimeyer, 1873; Bräm, 1965; Karl et al., 2007; Anquetin, Deschamps & Claude, 2014,
- Anquetin, Püntener & Billon-Bruyat, 2014; Anquetin, Püntener & Billon-Bruyat, 2015; Anquetin
- & Chapman, 2016). Plesiochelys planiceps (Owen, 1842), the only other valid species in the
- 54 genus, is known only from a single specimen (cranium, mandibule, and remains of the hyoids
- and cervical vertebrae) from the Tithonian of the Isle of Portland, UK. The cranium of *Pl.*



planiceps differs in many aspects from that of Pl. etalloni (Anguetin, Püntener & Billon-Bruyat, 2015). 57 In the present study we describe new material of *Plesiochelys* from the Kimmeridgian of 58 Porrentruy, Canton Jura, Switzerland. The new specimens were found by the Paleontology A16 59 project, which rescued the paleontological material discovered during the construction of the 60 61 A16 Transjurane highway. These excavations yielded a great number of fossil vertebrates from Kimmeridgian layers, notably including dinosaur trackways (Marty & Hug, 2003; Marty et al., 62 2007; Marty, 2008; Marty & Billon-Bruyat, 2009) and numerous coastal marine turtles (Billon-63 Bruyat, 2005a). The rich and diverse turtle fauna from Porrentruy notably includes different 64 species of Plesiochelyidae and Thalassemydidae (see Geological setting) (Püntener et al., 2014; 65 Anguetin, Püntener & Billon-Bruyat, 2015; Püntener, Anguetin & Billon-Bruyat, 2015). 66 As in Solothurn, *Plesiochelys* is by far the most common turtle taxon in the Kimmeridgian 67 of Porrentruy. Slightly more than 100 relatively complete, but mostly disarticulated shells were 68 69 discovered during the excavations, out of which 80 can be referred to *Plesiochelys*. Among these shells, 41 are herein assigned to a new species, *Plesiochelys bigleri* n. sp. We furthermore refer 70 15 shells to *Plesiochelys etalloni*, and 24 shells to *Plesiochelys* sp. This material is described in 71 72 detail herein. The shell of *Pl. bigleri* shows only minor anatomical differences with that of *Pl.* etalloni, but cranial anatomy clearly distinguishes the two species. Two skulls, one associated 73 74 with a shell and the other found isolated, are known for *Pl. bigleri*. A statistical analysis confirms 75 that the thickness of neural bones allows to separate the two species and to tentatively identify otherwise indeterminate specimens. Based on abundant shell material, the intraspecific variations 76 77 in both species are discussed in details. Finally, we fully describe and illustrate elements of the



| 78  | appendicular skeleton, which are otherwise rarely described in the literature, hoping that this will       |
|-----|--|
| 79  | facilitate future comparisons.   |
| 80  |  |
| 81  | MATERIAL AND METHODS   |
| 82  |  |
| 83  | Material   |
| 84  | The present study is based on a collection of 80 relatively complete, but mostly disarticulated            |
| 85  | shells (Table 1), most of which were found in a single stratigraphical layer (see Geological               |
| 86  | setting, below). Forty-one shells are referred to a new species, <i>Plesiochelys bigleri</i> n. sp. One of |
| 87  | these specimens (MJSN TCH007-252) is a skull-shell association, which we designate as the                  |
| 88  | holotype of the new species. An isolated cranium (MJSN TCH006-1451) is also referred to this               |
| 89  | new species and designated as its paratype.  |
| 90  | Fifteen out of the 80 aforementioned shells are identified as <i>Plesiochelys etalloni</i> . The           |
| 91  | identification of the remaining 24 shells is uncertain because they lack diagnostic features. These        |
| 92  | specimens are therefore referred to <i>Plesiochelys</i> sp. However, a tentative identification of some    |
| 93  | of these specimens is provided herein based on the statistical analysis of neural bone thickness           |
| 94  | (see below).   |
| 95  |  |
| 96  | Geological setting   |
| 97  | All of the specimens were collected between 2001 and 2011 near the small town of Courtedoux,               |
| 98  | along the A16 Transjurane highway in the Ajoie Region, Canton of Jura, NW Switzerland (Fig.                |
| 99  | 1). The majority of the specimens come from the Lower Virgula Marls (Reuchenette Formation,                |
| 100 | Chevenez Member; Comment et al., 2015) of the sites of Bois de Sylleux (BSY), Sur Combe                    |
|     |  |



| 101 | Ronde (SCR), and Tchâfouè TH) (Fig. 2). These sites yielded a rich and diverse coastal                  |
|-----|---|
| 102 | marine assemblage, including invertebrates (bivalves, gastropods, cephalopods, crustaceans, and         |
| 103 | echinoderms), vertebrates (chondrichthyans, osteichthyans, turtles, crocodilians, and pterosaurs),      |
| 104 | and wood remains (e.g., Billon-Bruyat, 2005a; Billon-Bruyat, 2005b; Marty & Billon-Bruyat,              |
| 105 | 2009; Philippe et al., 2010; Schaefer, 2012; Comment et al., 2015; Koppka, 2015; Leuzinger et           |
| 106 | al., 2015).   |
| 107 | Plesiochelys is the dominating turtle taxon in the Lower Virgula Marls. Other taxa occur                |
| 108 | only in small numbers, including <i>Tropidemys langii</i> Rütimeyer, 1873, <i>Portlandemys gracilis</i> |
| 109 | Anquetin, Püntener & Billon-Bruyat, 2015, Thalassemys hugii Rütimeyer, 1873, and                        |
| 110 | Thalassemys bruntrutana Püntener, Anquetin & Billon-Bruyat, 2015 (Püntener et al., 2014;                |
| 111 | Anquetin, Püntener & Billon-Bruyat, 2015; Püntener, Anquetin & Billon Bruyat, 2015). The                |
| 112 | Lower Virgula Marls are dated from the Eudoxus ammonite zone (early late Kimmeridgian;                  |
| 113 | Comment et al., 2015) and are therefore slightly older than the Solothurn Turtle Limestone,             |
| 114 | which forms the uppermost member of the Reuchenette Formation and is dated from the                     |
| 115 | Autissiodorensis ammonite zone (Meyer, 1994; Comment, Ayer & Becker, 2011).                             |
| 116 | One specimen of Plesiochelys bigleri (MJSN CRT007-2) has been discovered within the                     |
| 117 | dinosaur track-bearing tidal laminites of the Crat site (CRT; Fig. 2) (Billon-Bruyat et al., 2012).     |
| 118 | These laminites represent the lowermost layers of the Corbis Limestones and are dated from the          |
| 119 | Cymodoce ammonite zone (late early Kimmeridgian; Comment et al., 2015). Two other                       |
| 120 | specimens of Plesiochelys bigleri (MJSN VTT006-299 and MJSN VTT006-579) are                             |
| 121 | stratigraphically slightly older and come from the Banné Marls of the Vâ Tche Tchâ site (VTT;           |
| 122 | Cymodoce ammonite zone; Fig. 2), where <i>Tropidemys langii</i> is the dominating turtle taxon          |
| 123 | (Püntener et al., 2014).  |



Most turtle shells from Porrentruy have been discovered in a state of partial disarticulation, which contrasts with the mostly articulated shells found in Solothurn. The latter were apparently rapidly incorporated in a calcareous mud, while the turtle remains from Porrentruy remained for a longer period on top of the sediment before being completely buried. This is confirmed by the common presence of incrusting bivalves (oysters) on the bone remains from Porrentruy. However, disturbance by predators or water movements was relatively limited since disarticulated elements were usually found relatively close together (Fig. 3).

### **Anatomical comparisons**

As far as the cranium is concerned, *Plesiochelys bigleri* was compared to all plesiochelyids for which that part of the skeleton is known: *Plesiochelys etalloni* (NMB 435, NMS 8738, NMS 8739, NMS 8740, NMS 9145, NMS 40870, NMS 40871, NHMUK R3370), *Plesiochelys planiceps* (OUMNH J.1582), *Portlandemys mcdowelli* Gaffney, 1975a (NHMUK R2914, NHMUK R3164), and *Portlandemys gracilis* (MJSN BSY009-708). When pertinent, comparisons were also extended to PIMUZ A/III 514, a skull-shell association from the Tithonian of the Isle of Oléron (Department of Charente-Maritime, France) initially referred to *Thalassemys moseri* Bräm, 1965 by Rieppel (1980), but which was recently designated as the holotype of a new taxon, *Jurassichelon oleronensis* Pérez-García, 2015. All of these specimens have been studied first hand by the second author. The reader is referred to the primary literature describing these specimens (Parsons & Williams, 1961; Gaffney, 1975a; Gaffney, 1976; Rieppel, 1980; Anquetin, Püntener & Billon-Bruyat, 2015; Anquetin & Chapman, 2016). Anatomical descriptions in the present study follow the nomenclature established by Gaffney (1972, 1979) as updated by Rabi et al. (2013).





Anatomical descriptions of shell material follow the nomenclature established by Zangerl (1969). Shell and non-shell postcranial material of *Pl. bigleri* was compared, when pertinent, to plesiochelyids (*Plesichelys etalloni, Tropidemys langii*, and *Craspedochelys jaccardi*) and thalassemydids (*Thalassemys bruntrutana* and *Thalassemys hugii*).

### Statistical analysis

The length and thickness of 119 neurals 2 to 5 pertaining to 43 selected specimens (25 *Plesiochelys bigleri*, 8 *Plesiochelys etalloni*, and 10 *Plesiochelys* sp.) were measured in order to test the hypothesis that neural bones are significantly thinner in *Pl. bigleri* relative to *Pl. etalloni* (see Table S1). Length was measured as the maximal length on the dorsal surface of the neural bone. Thickness was measured on the left and right sides and approximately at the mid-length of each neural bone (see below). The mean of these two measurements was used as the thickness value for each individual neural bone (Table S1). Measurements were taken using a digital Vernier caliper by a single operator (CP).

Neural shape can be relatively variable within a single individual. For example, one neural can be disproportionately shorter, longer, thinner, or thicker in a given neural series. Specimens exhibiting extreme divergences from the common condition were not measured. For specimens included in this analysis, the mean neural length and mean neural thickness were computed for each individual, which had the effect of smoothing intra-individual discrepancies. The analyzed dataset therefore consists of the mean neural length, mean neural thickness, and corresponding length/thickness ratio measured for the 43 included specimens (see below).

The statistical analysis was run using PAST 3.14 (Hammer, Harper & Ryan, 2001). Length and thickness were plotted in a 2D space, whereas length, thickness, and length/thickness ratio





| 170 | were tested for equal medians using a non-parametric Mann-Whitney test (with Monte Carlo   |
|-----|--|
| 171 | permutations). A discriminant analysis was also performed on the length and thickness  |
| 172 | measurements and used to tentatively identify indeterminate specimens (Plesiochelys sp.; see   |
| 173 | below).  |
| 174 |  |
| 175 | 3D Models  |
| 176 | 3D models of the holotype (MJSN TCH007-252) and paratype (MJSN TCH006-1451) crania   |
| 177 | have been computed with the photogrammetry software Agisoft Photoscan 1.0.4 Standard   |
| 178 | Edition using sets of high-quality photographs of the specimens. We followed the procedures  |
| 179 | recently described by Mallison & Wings (2014). These models are provided herein as 3D PDFs   |
| 180 | (reduced resolution; to be opened with Adobe Acrobat): MJSN TCH007-252 (Fig. S1), and  |
| 181 | MJSN TCH006-1451 (Fig. S2). Scaled and textured high-resolution meshes in PLY format are   |
| 182 | also available freely on figshare ( <a href="http://figshare.com/authors/J_r_my_Anquetin/651097">http://figshare.com/authors/J_r_my_Anquetin/651097</a> ). |
| 183 | A 3D surface scan of the pelvis preserved with specimen MJSN BSY006-307 was  |
| 184 | produced with an Artec Space Spider scanner (Artec Group, Luxembourg;  |
| 185 | http://www.artec3d.com) and reconstructed with Artec Studio 10, the native scanner software.   |
| 186 | The textured 3D mesh in PLY format is freely available on figshare   |
| 187 | (http://figshare.com/authors/J_r_my_Anquetin/651097).  |
| 188 |  |
| 189 | Nomenclatural act  |
| 190 | The electronic version of this article in Portable Document Format (PDF) will represent a  |
| 191 | published work according to the International Commission on Zoological Nomenclature (ICZN),  |
| 192 | and hence the new name contained in the electronic version is effectively published under that   |
|     |  |



| 193 | Code from the electronic edition alone. This published work and the nomenclatural act it   |
|-----|--|
| 194 | contains have been registered in ZooBank, the online registration system for the ICZN. The                                       |
| 195 | ZooBank LSIDs (Life Science Identifiers) can be resolved and the associated information viewed                                   |
| 196 | through any standard web browser by appending the LSID to the prefix <a href="http://zoobank.org/">http://zoobank.org/</a> . The |
| 197 | LSID for this publication is: urn:lsid:zoobank.org:pub:C5AE9DE8-9911-4CFD-AD09-  |
| 198 | 65850C35BDEC. The online version of this work is archived and available from the following                                       |
| 199 | digital repositories: PeerJ, PubMed Central and CLOCKSS.   |
| 200 |  |
| 201 | SYSTEMATIC PALEONTOLOGY  |
| 202 | TESTUDINES Batsch, 1788  |
| 203 | PAN-CRYPTODIRA Joyce, Parham & Gauthier, 2004  |
| 204 | EUCRYPTODIRA Gaffney, 1975c  |
| 205 | PLESIOCHELYIDAE Baur, 1888   |
| 206 | Plesiochelys Rütimeyer, 1873   |
| 207 | Type species. Plesiochelys solodurensis Rütimeyer, 1873  |
| 208 | Included valid species. Plesiochelys planiceps (Owen, 1842); Plesiochelys etalloni (Pictet &                                     |
| 209 | Humbert, 1857); Plesiochelys bigleri n. sp.  |
| 210 | Referred material and range. Kimmeridgian of Switzerland, France, Germany, and England   |
| 211 | (Pictet & Humbert, 1857; Maack, 1869; Rütimeyer, 1873; Oertel, 1924; Bräm, 1965; Karl et al.,                                    |
| 212 | 2007; Anquetin, Deschamps & Claude, 2014; Anquetin, Püntener & Billon-Bruyat, 2014;  |
| 213 | Anquetin, Püntener & Billon-Bruyat, 2015; Anquetin & Chapman, 2016), and Tithonian of  |
| 214 | England (Owen, 1842; Gaffney 1975a; Gaffney, 1976; Anquetin, Püntener & Billon-Bruyat,   |
| 215 | 2015). Indeterminate specimens are also signalled from the Kimmeridgian-Tithonian of Portugal                                    |



| 216 | (Pérez-García et al., 2008) and late Tithonian of Spain (Pérez-García, Scheyer & Murelaga,     |
|-----|--|
| 217 | 2013).   |
| 218 | Diagnosis. See Anquetin, Püntener & Billon-Bruyat (2014, 2015).                                |
| 219 |  |
| 220 | Plesiochelys etalloni (Pictet & Humbert, 1857)   |
| 221 | Synonymy. Emys Etalloni Pictet & Humbert, 1857 (original description); Stylemys hannoverana    |
| 222 | Maack, 1869 (subjective synonymy); Plesiochelys langii Rütimeyer, 1873 (subjective             |
| 223 | synonymy); Plesiochelys sanctaeverenae Rütimeyer, 1873 (subjective synonymy); Plesiochelys     |
| 224 | solodurensis Rütimeyer, 1873 (subjective synonymy); Plesiochelys solodurensis var.             |
| 225 | langenbergensis Oertel, 1924 (subjective synonymy).  |
| 226 | Type material. MAJ 2005-11-1, a shell missing a large part of the carapace medially.           |
| 227 | Illustrations of type. Pictet & Humbert (1857: plates I-III); Anquetin, Deschamps & Claude     |
| 228 | (2014: Figs. 1 and 2, S2); Anquetin, Püntener & Billon-Bruyat (2014: Figs. 2A-2D).             |
| 229 | Type horizon and locality. "Forêt de Lect" (Lect is a small village) near Moirans-en-Montagne  |
| 230 | (Department of Jura, France), Late Jurassic. See Anquetin, Deschamps & Claude (2014) for       |
| 231 | details.   |
| 232 | Referred material and range. Kimmeridgian of Oker and Hannover, Lower Saxony, Germany          |
| 233 | (Maack, 1869; Oertel, 1924; Karl et al., 2007); Kimmeridgian of Solothurn, Canton of Solothurn |
| 234 | and Glovelier and Porrentruy, Canton of Jura, Switzerland (Rütimeyer, 1873; Bräm, 1965;        |
| 235 | Gaffney, 1975a; Gaffney, 1976; Anquetin, Deschamps & Claude, 2014; Anquetin, Püntener &        |
| 236 | Billon-Bruyat, 2014; Anquetin, Püntener & Billon-Bruyat, 2015; Table 1); Kimmeridgian of       |
| 237 | England, UK (Anquetin & Chapman, 2016).  |



239

240

241

242

243

244

245

246

247

248

249

250

251

252

253

Emended diagnosis. Plesiochelys etalloni differs from other Plesiochelys spp. in a more extensive flooring of the cavum acustico-jugulare by the pterygoid, the complete ossification of the pila prootica, and a narrow, slit-like foramen nervi trigemini. In addition, *Plesiochelys* etalloni differs from Plesiochelys planiceps in a smaller size, a lower lingual ridge on the maxilla, a narrower distance between the lingual ridges of the maxilla at the level of the pterygoid-vomer suture, a more rounded foramen palatinum posterius, a parietal-quadrate contact posterior to the foramen nervi trigemini, a less developed processus trochlearis oticum, a superficial canalis caroticus internus often remaining partly open ventrally, an absent or reduced contribution of the exoccipital to the condylus occipitalis, and the anterior portion of the lingual ridge on the dentary curving medially, and from *Plesiochelys bigleri* in a higher temporal skull roof, a deeper pterygoid fossa, a more developed processus trochlearis oticum, an anterior foramen nervi abducentis opening more posteriorly relative to the base of the processus clinoideus, foramina anterius canalis carotici cerebralis opening almost vertically below the dorsum sellae and usually more closely set, a processus paroccipitalis extending mainly posteriorly, an increased neural and costal bone thickness, the presence of epiplastral bulbs, and a more rounded or pointed anterior margin of the anterior plastral lobe.

254

255

256

258

259

260

### Plesiochelys bigleri sp. nov.

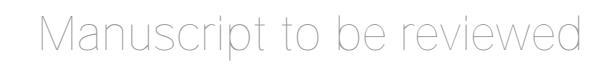
urn:lsid:zoobank.org:act:9A8EF46E-7DAA-4F5B-B727-58C559BA503C

257 Figs. 3–8, 9A–B, 10–15

Etymology. This species is dedicated to Pierre Bigler (Villars-sur-Fontenais, Canton of Jura,

Switzerland) who so skillfully prepared many of the fossil turtles from the Paleontology A16

collection, including the holotype specimen.





| 261 | Holotype. MJSN 1CH007-252, near complete disarticulated carapace, epiplastra, entoplastron,                  |
|-----|--|
| 262 | hypoplastra, and right xiphiplastron; basonium; proximal part of right scapular process;                     |
| 263 | proximal parts of both humeri; one radius; one ulna; both ilia with acetabulum (Figs. 4, 7, 11,              |
| 264 | and 12).   |
| 265 | Type locality and horizon. Tchâfoué (TCH), Courtedoux, near Porrentruy, Canton of Jura,                      |
| 266 | Switzerland. Lower Virgula Marls, Chevenez Member, Reuchenette Formation, late                               |
| 267 | Kimmeridgian, Late Jurassic (Comment, Ayer & Becker, 2011; Comment et al., 2015).                            |
| 268 | Paratype. MJSN TCH006-1451, an isolated partial cranium (Figs. 5 and 6).                                     |
| 269 | Referred material and range. Late early and early late Kimmeridgian of Porrentruy, Canton of                 |
| 270 | Jura, Switzerland (See Table 1).   |
| 271 | Diagnosis. Plesiochelys bigleri differs from other Plesiochelys spp. in a lower temporal skull               |
| 272 | roof, a shallower pterygoid fossa, a reduced processus trochlearis oticum, a more rounded                    |
| 273 | foramen nervi trigemini, an anterior foramen nervi abducentis opening anteromedially to the                  |
| 274 | base of the processus clinoideus, and foramina anterius canalis carotici cerebralis opening more             |
| 275 | anteriorly relative to the level of the dorsum sellae. In addition, <i>Plesiochelys bigleri</i> differs from |
| 276 | Plesiochelys planiceps in a smaller size, a lower lingual ridge on the maxilla, a parietal-quadrate          |
| 277 | contact posterior to the foramen nervi trigemini, a less developed processus trochlearis oticum, a           |
| 278 | superficial canalis caroticus internus that may have remained partly open ventrally, and an absen            |
| 279 | or reduced contribution of the exoccipital to the condylus occipitalis, and from Plesiochelys                |
| 280 | etalloni in a less extensive flooring of the cavum acustico-jugulare by the pterygoid, the absence           |
| 281 | of complete ossification of the pila prootica, a processus paroccipitalis extending                          |
| 282 | posterolaterally, a reduced neural and costal bone thickness, absent or poorly developed                     |
| 283 | epiplastral bulbs, and a more quadrangular anterior margin of the anterior plastral lobe.                    |



| 284 | Remarks. The better part of the 42 specimens referred to Plesiochelys bigleri will be amply                       |
|-----|---|
| 285 | illustrated in the forthcoming "Catalogues du patrimoine paléontologique jurassien", which                        |
| 286 | document the numerous discoveries made by the Paleontology A16 team. Hence, the present                           |
| 287 | study concentrates on illustrating the most significant specimens only.   |
| 288 |   |
| 289 | Plesiochelys sp.  |
| 290 | Referred material. Early late Kimmeridgian of Porrentruy, Canton of Jura, Switzerland (See                        |
| 291 | Table 1).   |
| 292 | Remarks. Twenty-four shells among the 80 studied herein lack sufficient diagnostic characters to                  |
| 293 | be clearly identified as either <i>Plesiochelys bigleri</i> or <i>Plesiochelys etalloni</i> . This is no surprise |
| 294 | considering how close these two species are in terms of shell anatomy. These 24 indeterminate                     |
| 295 | specimens are therefore provisionally referred to <i>Plesiochelys</i> sp. Ten of these indeterminate              |
| 296 | specimens are however tentatively identified herein based on a statistical analysis of neural bone                |
| 297 | thickness (see below).  |
| 298 |   |
| 299 | DESCRIPTION OF PLESIOCHELYS BIGLERI   |
| 300 |   |
| 301 | Cranium   |
| 302 |   |
| 303 | General description. The cranium of <i>Plesiochelys bigleri</i> is known from two specimens. The                  |
| 304 | first one is the holotype specimen (MJSN TCH007-252) and consists of the posterior part of a                      |
| 305 | skull (Fig. 4) associated with a relatively complete shell and some limb and girdle elements. The                 |
| 306 | parts of the skull anterior to the pterygoids (including the nasal, palatal, and orbital regions) and             |



the lateral part of the left otic chamber are missing. For this reason, the following bones are missing from that specimen: nasal, prefrontal, frontal, postorbital, premaxilla, maxilla, vomer, and palatine. Post-mortem deformation is minor, but the basicranium is partly disarticulated along the basisphenoid-pterygoid suture. The preservation of this specimen is not optimal. The skull was initially heavily encrusted by ferruginous mineralizations. Although most of these mineralizations were skillfully removed during preparation, sutures remain rather difficult to see in this specimen. The length of the skull as measured from the pterygoid-vomer suture to the stem of the condylus occipitalis (the condyle itself is missing) is 38.5 mm, whereas the width at the level of the condyli mandibularis is 60.6 mm (Table 2).

The second specimen (MJSN TCH006-1451) is an isolated, partial skull missing all of the skull roof, the ethmoid region, the orbital area, the anterior part of the snout, and most of the palate (Fig. 5). As a result, the following bones are missing from that specimen: nasal, prefrontal, frontal, postorbital, and premaxilla. The skull has been severely flattened dorsoventrally during fossilization. Crushing forces were not oriented exactly dorsoventrally and resulted in a slight lean toward the right hand side, mostly apparent in posterior view (Figs. 5E–5F). As preserved, the skull is 59.8 mm in length from the anteriormost part of the maxilla to the condylus occipitalis (34.4 mm from pterygoid-vomer suture to condylus occipitalis; see Table 2). The width taken at the level of the condyli mandibularis is 60 mm. MJSN TCH006-1451 is therefore slightly smaller than the holotype specimen (Table 2). Compared to other plesiochelyids, MJSN TCH006-1451 is about the same size as NMS 8738 and NMS 9145, both referred to *Plesiochelys etalloni*, but it is much smaller than OUMNH J.1582, the holotype skull of *Plesiochelys planiceps* (Anquetin, Püntener & Billon-Bruyat, 2015: table 1).



331

332

333

334

335

336

337

338

339

340

341

342

343

344

345

346

347

348

349

350

351

352

Parietal. The parietals are best preserved in the holotype specimen (MJSN TCH007-252), but fragments of the ventral part of the processus inferior parietalis are preserved on the right hand side of the paratype specimen (MJSN TCH006-1451). The parietals form the posterior part of the skull roof and meet one another medially (Fig. 4). The anterior and lateral contacts of the parietals are not preserved. Most of the posterior margin of each parietal is natural. The temporal skull roof is relatively low compared to other *Plesiochelys* spp. The upper temporal emargination largely exposes the foramen stapedio-temporale in dorsal view, but does not extend as far anteriorly as to expose the processus trochlearis oticum. This is similar to the condition in Pl. etalloni (NMB 435, NMS 40870). The development of the upper temporal emargination is not well known in other plesiochelyids. The preservation of the dorsal surface of the parietals in the holotype (MJSN TCH007-252) does not allow to identify scute sulci with confidence. As usual in plesiochelyids (Anguetin, Püntener & Billon-Bruyat, 2015), the anterior braincase wall formed mostly by the processus inferior parietalis is shorter than in most turtles as a result of the great development of the foramen interorbitale. As preserved, the ventral contacts of the parietal in *Pl. bigleri* are as follows: epipterygoid and pterygoid anterior to the foramen nervi trigemini; pterygoid, quadrate and prootic posterior to the foramen nervi trigemini; and supraoccipital posteroventrally (Figs. 4I–4L). The parietal forms the dorsal half of the anterior margin of the foramen nervi trigemini. There, the parietal and pterygoid have a broad contact that excludes the epipterygoid from the margin of that foramen. The posterior margin of the foramen nervi trigemini is formed entirely by a posteroventral process of the parietal that reaches the quadrate and prevents a contact between the pterygoid and prootic. This configuration of the region of the foramen nervi trigemini is characteristic of plesiochelyids (except for the parietalquadrate contact that is absent in *Pl. planiceps*) and *Jurassichelon oleronensis* (Anquetin,





| 353 | Püntener & Billon-Bruyat, 2015). In <i>Pl. bigleri</i> , the foramen nervi trigemini is somewhat more |
|-----|---|
| 354 | rounded than in other plesiochelyids, in which the foramen is usually taller than wide and oval in    |
| 355 | shape. In most specimens of Pl. etalloni (NMB 435, NMS 8738, NMS 40870, NMS 40871,                    |
| 356 | NHMUK R3370), the foramen nervi trigemini is very narrow and forms a slit-like opening.               |
| 357 |   |
| 358 | Jugal. In the holotype specimen (MJSN TCH007-252), the anterior part of the right jugal is            |
| 359 | preserved as an isolated fragment. A small flake of bone (probably from the maxilla) is still         |
| 360 | attached to the ventromedial margin of the isolated jugal. In the paratype specimen (MJSN             |
| 361 | TCH006-1451), only the ventral part of the jugal is preserved, but the bone is more complete on       |
| 362 | the right hand side (Fig. 5). The jugal forms the posteroventral corner of the orbit and contacts     |
| 363 | the maxilla ventrally and the quadratojugal posteriorly. The other contacts of the jugal with         |
| 364 | surrounding elements are unclear. As in Pl. etalloni, Pl. planiceps, and J. oleronensis, the jugal    |
| 365 | lacks a medial process extending to meet the pterygoid and/or palatine. Similarly, the maxilla        |
| 366 | lacks a corresponding posteromedial process and the foramen palatinum posterius remains open          |
| 367 | posterolaterally. The ventral margin of the jugal and the posterior border of the maxilla show that   |
| 368 | the lower temporal emargination was relatively well developed in Pl. bigleri, much like the           |
| 369 | condition in Pl. etalloni, Pl. planiceps and J. oleronensis (note that the condition in               |
| 370 | Portlandemys spp. is unknown).  |
| 371 |   |
| 372 | Quadratojugal. The morphology of the quadratojugal is poorly known in Pl. bigleri. Only a             |
| 373 | small part of the right quadratojugal is preserved anterior to the cavum tympani in the holotype      |
| 374 | (MJSN TCH007-252). A larger portion of the right quadratojugal is preserved in the paratype           |
| 375 | (MJSN TCH006-1451), but the bone is fragmented in several pieces and misses its dorsal and            |
|     |   |





anterior margins. Anteriorly, the quadratojugal articulates with the jugal. Its ventral margin forms the posterior half of the lower temporal emargination. Posteriorly, the quadratojugal braces the external margin of the cavum tympani along an extended, curved suture with the quadrate (Figs. 4 and 5). It seems that the posteroventral process of the quadratojugal along the processus articularis of the quadrate is proportionally shorter in *Pl. bigleri* than in *Pl. etalloni* and *Po. gracilis* (unknown in other plesiochelyids). Posterodorsally, the quadratojugal has a broad vertical contact with the squamosal just dorsal and slightly anterior to the level of the incisura columellae auris.

**Squamosal.** The squamosal is best preserved in the holotype (MJSN TCH007-252), but the paratype (MJSN TCH006-1451) provides additional information on the morphology of this element. As usual in turtles, the squamosal forms the posterolateral corner of the otic chamber, notably contributing to the formation of the antrum postoticum. The anterodorsal part of the bone is unfortunately not preserved in any specimen. The contacts of the squamosal in the temporal roof (notably with the postorbital and parietal) are therefore unknown in *Pl. bigleri*. The other contacts of the squamosal are as follows: quadrate anteromedially and ventrally; quadratojugal anterolaterally; and opisthotic posteromedially. Compared to other turtles, the antrum postoticum of plesiochelyids is usually described as moderately developed (Gaffney, 1976; Rieppel, 1980; Anquetin, Püntener & Billon-Bruyat, 2015). In *Pl. bigleri*, the antrum postoticum is also moderately developed, but, compared to other plesiochelyids, the cavity is deeper both medially and posterodorsally. Remarkably, the anterior margin of the antrum postoticum is formed entirely by the quadrate (MJSN TCH007-252; Fig. 4). This differs from the condition observed in *Pl. etalloni* and *Po. gracilis* (as well as *J. oleronensis* and most basal pan-cryptodires) in



which the squamosal contributes to the anterolateral margin of the antrum postoticum. The posterodorsal parasagittal crest of the squamosal is well developed in *Pl. bigleri*, notably the 400 posterior part that forms an extended and somewhat pointed lamina (MJSN TCH007-252; Figs. 401 4I–4J). A wide concavity is present on the lateral surface of the squamosal just posterior to the 402 opening of the antrum postoticum. Posteroventrally, the squamosal contributes only to a limited 403 404 extent to the rugose area for the attachment of the M. depressor mandibulae (Werneburg, 2011). 405 **Maxilla.** The maxilla is not preserved in the holotype specimen. Only the posterior part of the 406 bone is preserved in the paratype (MJSN TCH006-1451), but about half of the original bone is 407 present on the right hand side in that specimen (Fig. 5). As preserved, the maxilla contacts the 408 jugal posterodorsally and the palatine posteromedially. As for the jugal, the maxilla lacks a 409 posteromedial process that would close the foramen palatinum posterius posterolaterally. The 410 maxilla seems to participate to the anterolateral margin of the foramen palatinum posterius both 411 412 in dorsal and ventral views. The labial ridge is slender and very high, notably posteriorly. Anteriorly, the labial ridge is somewhat blunted in MJSN TCH006-1451, but this is possibly a 413 preservational artifact. The labial ridge is separated from the lingual ridge by a deep trough. As 414 415 in Pl. etalloni, Pl. planiceps, and Po. mcdowelli (unknown in Po. gracilis), the lingual ridge is broad and high. In these species, the lingual ridge is rugose, which contrasts with the condition in 416 417 J. oleronensis where the summit of the lingual ridge is acute and smooth. In Pl. bigleri, the 418 lingual ridge is closer to the condition in other plesiochelyids, but the bone surface is slightly eroded. In contrast to Po. mcdowelli, the lingual ridge is formed entirely by the maxilla. Due to 419 420 poor preservation and the presence of markings on the bone surface, we were unable to locate the 421 foramen supramaxillare in MJSN TCH006-1451.

| 400 | 1 | 1 | 1 |
|-----|---|---|---|

**Vomer.** The vomer is missing in the holotype (MJSN TCH007-252) and only the posteroventral part of the bone is preserved in MJSN TCH006-1451 (only visible in ventral view). Posteriorly, the vomer reaches the pterygoids and fully separates the palatines on the ventral surface of the palate, but not on the dorsal surface (Fig. 5). This configuration is similar to that of *Pl. etalloni* and *Po. mcdowelli*, but differs from that of *J. oleronensis*. The condition in *Pl. planiceps* is uncertain because the posteroventral part of the vomer is broken in the type and only known specimen (OUMNH J.1582).

Palatine. The palatine is only preserved in the paratype (MJSN TCH006-1451). The bone is not complete and only the posterior and lateral parts can be observed (Fig. 5). As preserved, the palatine contacts the pterygoid posteriorly, the vomer medially on the ventral surface of the palate, the other palatine medially on the dorsal surface of the palate, and the maxilla anterolaterally. Laterally, the palatine defines the anteromedial border of the foramen palatinum posterius. The outline of the foramen palatinum posterius is impossible to assess in *Pl. bigleri* since the lateral margin of the palatine and anterolateral part of the pterygoid are incomplete in all of the specimens. The palatine was initially described as forming a small portion of the lingual ridge in *Plesiochelys* and *Portlandemys* (Gaffney, 1976). In fact, the palatine really contributes to the lingual ridge only in *Po. mcdowelli* (condition unknown in *Po. gracilis*). In *Pl. etalloni*, *Pl. bigleri*, *Pl. planiceps* and *J. oleronensis*, the palatine-maxilla suture extends along the medial base of the lingual ridge, i.e. on its dorsomedial edge, and the palatine therefore does not take part into the formation of the ridge or triturating surface.



| 445 | Quadrate. On the dorsal surface of the otic chamber, the quadrate contacts the prootic                        |
|-----|---|
| 446 | anteromedially, the opisthotic posteromedially, and the squamosal posterolaterally. As usual,                 |
| 447 | quadrate and prootic contribute relatively equally to the formation of the foramen stapedio-                  |
| 448 | temporale, but variability exists (see right side of the holotype MJSN TCH007-252).                           |
| 449 | Anterolaterally, the quadrate has a long curved suture with the quadratojugal. This suture is                 |
| 450 | mostly parallel to the anterior margin of the cavum tympani, but lies anterior to it (the                     |
| 451 | quadratojugal does not enter the margin of the cavum tympani). The cavum tympani of $Pl$ .                    |
| 452 | bigleri is deeper than in other plesiochelyids. This is notably apparent anteroventral and                    |
| 453 | posterodorsal to the incisura columellae auris. In contrast to other plesiochelyids, the lateral              |
| 454 | margin of the cavum tympani faces more posterolaterally than laterally in Pl. bigleri (Figs. 4 and            |
| 455 | 5). The quadrate forms the entire anterior margin of the antrum postoticum, which is remarkable               |
| 456 | (see Squamosal). The incisura columellae auris remains open posteroventrally. The processus                   |
| 457 | articularis of the quadrate is damaged in the holotype (MJSN TCH007-252), which may give the                  |
| 458 | misleading impression that this process is short. This structure is better preserved in the paratype          |
| 459 | (MJSN TCH006-1451). A prominent ventrally-infolding ridge occurs on the posterior surface of                  |
| 460 | the processus articularis. Starting from the posterolateral corner of the condylus mandibularis,              |
| 461 | this ridge extends dorsomedially toward the incisura columellae auris increasing in height.                   |
| 462 | Ventral to the incisura, the ridge thickens and bends sharply medially. Pursuing its medial                   |
| 463 | course, the ridge thins progressively and finally merges with the posterolateral border of the                |
| 464 | pterygoid. This ventrally-infolding ridge is found in all plesiochelyids, but also in <i>J. oleronensis</i> , |
| 465 | Solnhofia parsonsi Gaffney, 1975b and Parachelys eichstaettensis Meyer, 1864, and is a strong                 |
| 466 | argument to support the monophyly of these Late Jurassic coastal marine turtles from Europe                   |
| 467 | (Anquetin, Püntener & Billon-Bruyat, 2015). The condylus mandibularis of <i>Pl. bigleri</i> is                |





remarkably narrow anteroposteriorly compared to other plesiochelyids. The condyle consists of two slightly concave facets separated by a wide, but shallow parasagittal furrow.

The quadrate forms about half of the moderately developed processus trochlearis oticum, which is less prominent than in *Plesiochelys etalloni*. On the anterior surface of the otic chamber, the quadrate contacts the prootic dorsomedially, the parietal medially, and the pterygoid ventromedially. This region is best preserved on the left hand side of the holotype MJSN TCH007-252. Inside the cavum acustico-jugulare, the quadrate forms the lateral part of the aditus canalis stapedio-temporalis and canalis stapedio-temporalis, as well as the lateral half of the posterior opening of the canalis cavernosus. Below the antrum postoticum, a rugose area occurs on the ventral surface of the skull and probably served for muscular attachment. In *Pl. bigleri*, this area is mostly formed by the quadrate, with minor contributions from the opisthotic and squamosal.

Epipterygoid. The epipterygoid is best of vable in the holotype (MJSN TCH007-252), whereas only the ventral part of the bone is preserved in the paratype (MJSN TCH006-1451). In lateral view, the epipterygoid is a trapezoidal element located between the crista pterygoidea of the pterygoid and the processus inferior parietalis of the parietal. The epipterygoid is exposed on the medial surface of the anterior braincase wall, albeit to a more moderate extent. Posteriorly, a broad contact between the parietal and pterygoid excludes the epipterygoid from the anterior margin of the foramen nervi trigemini (Figs. 4I–4L). The same configuration seemingly occurs on the medial surface of the anterior braincase wall. Posteroventrally, a fossa cartilaginis epipterygoidei is present and prevents a contact between the epipterygoid and the quadrate. The anterolateral process of the epipterygoid that extends onto the dorsal surface of the pterygoid is



### **PeerJ**

513

well developed. A shallow furrow prolongs this process on the dorsal surface of the pterygoid in 491 Pl. bigleri (MJSN TCH006-1451). A similar process occurs in Pl. etalloni and Po. mcdowelli. 492 493 This process is more reduced in *Pl. planiceps* and *J. oleronensis*. 494 **Pterygoid.** Except for each processus pterygoideus externus, the pterygoids are complete in the 495 496 paratype (MJSN TCH006-1451), but their ventral surface is somewhat abraded. Longitudinal striae extend from the pterygoid fossae posteriorly to the palatines and vomer anteriorly (Fig. 497 5C). In the holotype (MJSN TCH007-252), the anterior part of the pterygoids is more poorly 498 preserved, although the left processus pterygoideus externus is complete. In contrast, the 499 posterior part of the pterygoids (pterygoid fossa and quadrate process) is better preserved. The 500 pterygoids are disarticulated from the basicranium in the holotype. 501 In ventral view, the pterygoid contacts the vomer anteromedially, the palatine anteriorly, 502 the quadrate posterolaterally, and the basisphenoid posteromedially. Posteriorly, the pterygoid 503 504 probably also contacted the basioccipital, but the sutures in this region are poorly preserved in both specimens. As preserved, the pterygoid does not seem to contact the exoccipital posteriorly, 505 but this region is rarely well preserved in plesiochelyids and the presence/absence of this contact 506 507 is probably of poor systematic value (Anguetin, Püntener & Billon-Bruyat, 2015). In ventral view, the processus pterygoideus externus is similar in development and shape to that of Pl. 508 509 etalloni and Pl. planiceps. However, the parasagittal plate on the lateral margin of the processus 510 pterygoideus externus is more developed in *Pl. etalloni* than in the two other species. A distinct ridge extends posteromedially from the posterior edge of the processus pterygoideus externus to 511 512 the posterolateral part of the ventrally open canalis caroticus internus. This ridge forms the

medial margin of the pterygoid fossa. Compared to other plesiochelyids, J. oleronensis and





515

516

517

518

519

520

521

522

523

524

525

526

527

528

529

530

531

532

533

534

535

536

eurysternids (Anquetin, Püntener & Billon-Bruyat, 2015), the pterygoid fossa of *Pl. bigleri* stands out as being remarkably shallow. The configuration of the canalis caroticus internus is similar to the condition in Pl. etalloni and J. oleronensis (see Anguetin, Püntener & Billon-Bruyat, 2015 for a review). The canalis caroticus internus is superficial and open ventrally at least along its anterior half (Figs. 4 and 5). The posterior half of the canalis caroticus internus may have been floored by a thin ventromedial flap of the pterygoid, but the preservation of the paratype (MJSN TCH006-1451) prevents a definitive conclusion. Since no flooring is preserved in any specimen, the position of the foramen posterius canalis carotici interni cannot be determined with precision. The anterior part of the canalis caroticus internus follows the basisphenoid-pterygoid suture. By comparison with *Pl. etalloni*, the split between the palatine and cerebral branches of the internal carotid artery was probably not floored by bone, but the preservation of the specimens prevents a clear observation of the foramen posterius canalis carotici palatinum (possibly visible on the left hand side of MJSN TCH006-1451) and foramen posterius canalis carotici cerebralis. The flooring of the cavum acustico-jugulare by the posterolateral part of the pterygoid is not very extensive. The processus interfenestralis of the opisthotic therefore remains largely visible in ventral view. For that matter, Pl. bigleri is closer to the condition observed in *Pl. planiceps*. Although this contact is now disarticulated in the holotype, there was a contact between the processus interfenestralis of the opisthotic and the pterygoid. Based on the disarticulated surface, this contact was probably not sutural. Lateral to this contact, the pterygoid forms the medial part of the floor of the posterior opening of the canalis cavernosus. In the ethmoid region, the pterygoid forms the ventral margin of the foramen nervi

trigemini, the rest of the foramen margin being formed by the parietal (Figs. 4I–4L). The





538

539

540

541

542

543

544

545

546

547

548

549

550

551

pterygoid-parietal contact anterior to the foramen nervi trigemini excludes the epipterygoid from the margin of this foramen. Medial to the crista pterygoidea, the pterygoid forms the floor of the sulcus cavernosus. This region is best preserved in the paratype specimen (MJSN TCH006-1451). The foramen anterius canalis carotici palatinum opens in the anterior part of the sulcus cavernosus about halfway between the level of the foramen anterius canalis carotici interni and the tip of the trabecula. After exiting the foramen anterius canalis carotici palatinum, the palatine branch of the internal carotid artery continues forward in a groove within the floor of the sulcus cavernosus and is not obstructed anteriorly by a crest extending from the crista pterygoidea to the midline shelf of the pterygoid, as seen in some plesiochelyids (Anquetin, Püntener & Billon-Bruyat, 2015). Anterolaterally, a small foramen occurs on the dorsal surface of the pterygoid medial to the anterolateral process of the epipterygoid. This foramen may correspond to the foramen nervi vidiani, but this should be further investigated (see also Anquetin, Püntener & Billon-Bruyat, 2015). Anterior to this small foramen, the dorsal surface of the pterygoid forms a shallow, rounded depression, which likely served for the attachment of one of the eye muscles (Gaffney, 1976). Finally, as noted above (see Epipterygoid), a shallow furrow prolongs the anterolateral process of the epipterygoid on the dorsal surface of the pterygoid. **Supraoccipital.** The supraoccipital contacts the parietal anteriorly, the prootic anterolaterally,

553

554

555

556

557

558

559

552

Supraoccipital. The supraoccipital contacts the parietal anteriorly, the prootic anterolaterally, the opisthotic posterolaterally, and the exoccipital posteriorly. A broad contact between the prootic and opisthotic separates the supraoccipital from the quadrate on the floor of the fossa temporalis superior (Figs. 4 and 5). This contrasts with the condition observed in *Po. mcdowelli* and most specimens referred to *Pl. etalloni*. Most of the crista supraoccipitalis is preserved in the holotype MJSN TCH007-252. This structure is relatively low, especially compared to *Pl.* 





planiceps and Po. mcdowelli. The condition in Pl. etalloni is more difficult to appreciate based 560 on the available material, but it seems to be intermediate in development between Pl. bigleri and 561 the two aforementioned species. The posterior part of the crista supraoccipitalis is broken in 562 MJSN TCH007-252, but it is unlikely that this structure projected far behind the level of the 563 condylus occipitalis. As usual, the supraoccipital forms the dorsal part of the foramen magnum. 564 565 **Exoccipital.** The exoccipital contacts the supraoccipital dorsomedially, the opisthotic 566 laterodorsally, the basioccipital ventrally, and the processus interfenestralis of the opisthotic 567 anterolaterally. As preserved, there is no contact between the exoccipital and pterygoid, which 568 may be a difference with *Pl. etalloni*, but this contact is often difficult to observe in this taxon 569 (Anguetin, Püntener & Billon-Bruyat, 2015). An exoccipital-pterygoid contact is otherwise 570 present in Portlandemys ssp. and J. oleronensis. In contrast to Pl. etalloni, Pl. planiceps, Po. 571 mcdowelli (condition unknown in Po. gracilis), and J. oleronensis, the exoccipitals apparently do 572 not meet in the floor of the foramen magnum, but this feature can present some intraspecific 573 variability (Anguetin & Chapman, 2016). The contribution of the exoccipital to the condylus 574 occipitalis is uncertain, but probably reduced. There are two foramina nervi hypoglossi on each 575 576 side and they are formed exclusively by the exoccipital. 577 578 **Basioccipital.** The ventral aspect of the basioccipital is poorly preserved in all specimens. 579 However, it is apparent that the basioccipital contacts the basisphenoid anteriorly and the pterygoid anterolaterally in this area. The tubercula basioccipitale are only moderately developed 580 581 and correspond to what is known in similarly-sized individuals of *Pl. etalloni*, but not in larger

specimens (Anguetin & Chapman, 2016). Posterodorsally, there is an extensive contact with the





exoccipital, but the basioccipital nevertheless enters the ventral margin of the foramen magnum. It appears that the basioccipital forms most of the condylus occipitalis, which is only preserved (poorly) in MJSN TCH006-1451. In dorsal aspect, the basioccipital offers little remarkable features. The basis tuberculi basalis is relatively low, and an oval depressed area occurs in front of it. Finally, there is also a contact with the ventromedial margin of the processus interfenestralis of the opisthotic in the floor of the recessus scalae tympani.

**Prootic.** On the dorsal surface of the otic chamber, the prootic contacts the parietal anteromedially, the quadrate laterally and anteroventrally, the opisthotic posteriorly, and the supraoccipital posteromedially. The prootic forms the medial half of the processus trochlearis oticum, which is reduced compared to that of *Pl. etalloni*. Anteromedially, the prootic is excluded from entering the posterior margin of the foramen nervi trigemini by an elongate descending process of the parietal (Figs. 4I–4L). A broad contact between this descending process of the parietal and the quadrate prevents a prootic-pterygoid contact in this area. This configuration is found in all plesiochelyids but *Pl. planiceps*, as well as in *J. oleronensis* and possibly also in eurysternids (Anquetin, Püntener & Billon-Bruyat, 2015).

Inside the cavum acustico-jugulare, the prootic forms the anterior half of the fenestra ovalis, the medial part of the aditus canalis stapedio-temporalis, and most of the roof of the posterior opening of the canalis cavernosus. As in other plesiochelyids, the aditus canalis stapedio-temporalis is located more posteriorly than the posterior opening of the canalis cavernosus rather than in the roof of the latter as in many turtles. In this area, the prootic contacts the opisthotic posterodorsally, the pterygoid ventrally, and the quadrate laterally. A C-shaped furrow occurs on the surface of the prootic dorsolateral to the fenestra ovalis. Inside the cavum



cranii, the prootic contacts the supraoccipital posterodorsally, the parietal anterodorsally, the basisphenoid ventromedially, and the pterygoid anteroventrally. In contrast to *Pl. etalloni*, the pila prootica is not ossified. Medial to the foramen nervi trigemini, the prootic forms a well-defined recess that accommodated the ganglion of the trigeminal (V) nerve.

Opisthotic. On the dorsal surface of the otic chamber, the opisthotic contacts the prootic anteriorly, the quadrate anterolaterally, the squamosal posterolaterally, the supraoccipital medially, and the exoccipital posteromedially. The anterior contact with the prootic is relatively wide and clearly separates the supraoccipital and quadrate (Figs. 4 and 5). This condition is found also in *Pl. planiceps*, *Po. gracilis*, and *J. oleronensis*. In contrast, the prootic-opisthotic contact is reduced or absent in *Po. mcdowelli* and most specimens of *Pl. etalloni*. The posterior aspect of the opisthotic is complete only on the right hand side of the paratype (MJSN TCH006-1451). The extremity of the processus paroccipitalis forms a distinct crest for muscular attachment. In *Pl. bigleri*, as well as in *Po. mcdowelli* and *J. oleronensis*, the processus paroccipitalis extends posterolaterally. This contrasts with *Pl. etalloni*, *Pl. planiceps*, and *Po. gracilis* in which the processus paroccipitalis extends more posteriorly. This difference changes the occipital outline as seen in dorsal view from a broad arch in *Pl. bigleri* to a more narrow arch in *Pl. etalloni*.

Ventrally, the opisthotic forms a large part of the roof of the cavum acustico-jugulare. In this area, the opisthotic contacts the prootic anteriorly, the quadrate anterolaterally, the squamosal posterolaterally, and the exoccipital posteromedially. The extremity of processus interfenestralis is triangular in shape and contacts the exoccipital, basioccipital, and pterygoid. The medial margin of the processus interfenestralis is pierced by a large fenestra perilymphatica,





630

631

632

633

634

635

which is apparently entirely contained in bone thanks to a ventromedial contribution from the basioccipital (MJSN TCH007-252). A well-defined foramen externum nervi glossopharyngei opens at the base of the processus interfenestralis. It is noteworthy that this foramen opens more laterally than in other plesiochelyids and *J. oleronensis*. Lateral to the base of the processus interfenestralis and foramen externum nervi glossopharyngei, the opisthotic forms a strong curving ridge oriented anteroposteriorly. As far as we know, this ridge is not present in other plesiochelyids.

636

637

638

639

640

641

642

643

644

645

646

647

648

649

650

651

**Basisphenoid.** In ventral aspect, the basisphenoid contacts the pterygoid anteriorly and laterally, and the basioccipital posteriorly (Figs. 4 and 5). As noted above, the basisphenoid-pterygoid suture is disarticulated in the holotype, but this contact is better preserved in the paratype (MJSN TCH006-1451). The posterior contact with the basioccipital is poorly preserved in both specimens. The general outline of the basisphenoid in ventral view is triangular, as in most plesiochelyids (Anguetin, Püntener & Billon-Bruyat, 2015). The ventral surface of the basisphenoid is apparently slightly concave. The morphology of the canalis caroticus internus is similar to the condition observed in *Pl. etalloni* and *J. oleronensis* (Anguetin, Püntener & Billon-Bruyat, 2015). The canalis caroticus internus is superficial and runs along the basisphenoidpterygoid suture as a ventrally open canal. The posterior part of the canalis caroticus internus may have been partly floored by a ventromedial flap formed by the pterygoid, but this region is not well preserved in any specimen. Based on the available material, the position of the foramen posterius canalis carotici interni cannot be determined. As in *Pl. etalloni*, the split between the cerebral and palatine branches of the internal carotid artery was probably not floored by bone. However, the preservation prevents a clear observation of the foramen posterius canalis carotici



653

654

655

656

657

658

659

660

661

662

663

664

665

666

667

668

669

670

671

672

673

674

anterior part of the basisphenoid. Anteriorly, these two canals penetrate deeply in the basisphenoid and exit in the sella turcica dorsally. A small unnamed foramen opens dorsomedially along the canalis caroticus cerebralis (only visible in MJSN TCH007-252; Fig. 4). The dorsal aspect of the basisphenoid is better preserved in the paratype (MJSN TCH006-1451) and can be readily observed in that specimen thanks to the loss of the anterior part of the roof of the cavum cranii (Fig. 6). The basioccipital contacts the basioccipital posteriorly, the prootic posterolaterally, and the pterygoid anterolaterally and anteriorly. The part of the basisphenoid that floors the cavum cranii is slightly concave. A moderately raised area located sagittally on the posterior margin of the basisphenoid corresponds to the anterior part of the basis tuberculi basalis. The posterior foramen nervi abducentis opens about midway along the part of the basisphenoid that floors the cavum cranii. The anterior foramen nervi abducentis opens ventral and slightly anteromedial to the base of the processus clinoideus, relatively close to the basisphenoid-pterygoid suture. This is the condition usually found in plesiochelyids, with the exception of Pl. etalloni (Anquetin, Püntener & Billon-Bruyat, 2015). The processus clinoideus is formed just medial to the basisphenoid-prootic suture. In contrast to *Pl. etalloni*, the pila prootica is not ossified. The dorsum sellae is high and does not overhang the sella turcica, as usual in plesiochelyids. The surface below the dorsum sellae is devoid of ridge and slopes relatively gently anteriorly. In that matter, Pl. bigleri is intermediate between Pl. etalloni, in which the surface below the dorsum sellae is near vertical, and *Portlandemys* spp., in which that surface slopes very gently anteriorly resulting in a relatively long distance between the dorsum sellae and the foramina anterius canalis carotici cerebralis (Anquetin, Püntener & Billon-Bruyat, 2015). The foramina anterius canalis carotici cerebralis are separated by a broad bar of bone,

palatinum. In the holotype, a portion of each canalis caroticus cerebralis is preserved on the



which is unusual in plesiocheyids, and open slightly posterior to the level of the foramina anterius canalis carotici palatinum. The trabeculae are relatively short and straight, and frame a small, well-defined sella turcica. The rostrum basisphenoidale is short, and the anterior tip of the trabeculae actually represents the anteriormost extension of the basisphenoid in dorsal view.

679

675

676

677

678

### Carapace

681

682

683

684

685

686

687

688

689

690

691

692

693

694

695

696

697

680

**General description.** Elements of the carapace are preserved in 39 out of the 41 shells herein referred to *Plesiochelys bigleri* (Figs. 7 and 8). The largest specimens reach a carapace length of about 550 mm (MJSN BSY006-307, MJSN SCR011-30, MJSN TCH005-21), whereas the smallest have a carapace length of about 220-250 mm (MJSN BSY008-848, MJSN SCR010-327, MJSN TCH007-516). Measuring carapace length with precision in disarticulated and incomplete specimens is not possible, but we estimate that most specimens are about 450 mm in carapace length, which corresponds approximately to what is known for *Pl. etalloni* in Solothurn. Most shells of *Pl. bigleri* are disarticulated, but two shells (MJSN BSY006-307 and MJSN TCH007-519) were found articulated. Bones were prepared out of the marly matrix individually and we were able to reassemble them on a moldable sand bed and reconstruct the 3D shape of the shell. Post-mortem deformation occurred in most specimens and to variable extents. Our reconstructions are therefore tentative. The resulting carapace outlines are either evenly oval (e.g., MJSN TCH006-767), or roundish (e.g., MJSN TCH007-252; Figs. 7A–7B). In some specimens the posterior carapace part is pointed (e.g., MJSN BSY009-815, MJSN SCR011-30). The shells of *Pl. bigleri* and *Pl. etalloni* are very similar. The following description therefore primarily focuses on the few differences between the two species and the intraspecific



variations observed in *Pl. bigleri*. A general description of the shell morphology of *Pl. etalloni* 698 and a discussion of its intraspecific variability can be found elsewhere (Anguetin, Deschamps & 699 Claude, 2014; Anguetin, Püntener & Billon-Bruyat, 2014). 700 701 **Nuchal.** The shape of the nuchal in *Pl. bigleri* varies from almost rectangular (e.g., MJSN 702 703 SCR011-140; Figs. 8I–8J) to trapezoidal (e.g., MJSN BSY007-257). This element can be about as wide as long (e.g., MJSN BSY009-815) or clearly wider than long (e.g., MJSN SCR011-160). 704 The nuchal notch is usually shallow, but can also be much reduced (e.g., MJSN SCR011-160) or 705 strongly pronounced (e.g., MJSN BSY007-257). In some specimens (e.g., MJSN TCH006-1420; 706 Figs. 8A–8B), the posteromedial part of the nuchal that articulates with the first neural projects 707 posteriorly. 708 709 Neurals, suprapygals and pygal. Like Pl. etalloni, Pl. bigleri usually has eight neurals, one 710 intermediate element, two suprapygals, and one pygal. However, this condition may vary. Neural 711 bones can be split in two (e.g., neural 2 in MJSN SCR010-342), fused together (e.g., neural 8 712 with the intermediate element in MJSN TCH005-21), or be reduced (e.g., neural 7 in MJSN 713 SCR011-140) or completely obliterated (e.g., neural 7 in MJSN SCR011-413 and MJSN 714 TCH006-1420; Figs. 8A-8B) by costals with midline contact. The first neural is rectangular to 715 716 oval in shape. It usually tapers posteriorly (not in MJSN BSY007-257 and MJSN TCH005-42; 717 Figs. 8M–8N). Neurals 2 to 6 are elongated hexagons with shorter sides facing anteriorly. However, these hexagons are often deformed (e.g., MJSN BSY007-257, MJSN SCR010-342, 718 719 MJSN SCR011-30, MJSN SCR011-276, MJSN SCR011-413, MJSN TCH005-42, MJSN 720 TCH006-767). Neurals 7 and 8 are shorter and more irregular in shape than the preceding





| 721 | neurals. Their growth is often constrained by a midline contact of the costals. Neural 8 is usually           |
|-----|---|
| 722 | the smallest bone in the series. In some specimens, it is pentagonal with shorter sides facing                |
| 723 | posteriorly (e.g., MJSN BSY009-815, MJSN TCH007-252; Figs. 7A-7B). The thickness of the                       |
| 724 | neural bones in <i>Pl. bigleri</i> is significantly reduced compared to <i>Pl. etalloni</i> (Fig. 9). This is |
| 725 | especially obvious for neurals 2 to 5. We statistically demonstrate this difference herein (see               |
| 726 | below).   |
| 727 | As relatively common in turtles (Zangerl, 1969), the posteromedial region of the carapace                     |
| 728 | is characterized by a great deal of intraspecific variation in Pl. bigleri. The element that follows          |
| 729 | neural 8 corresponds to the intermediate element of Anquetin, Püntener & Billon-Bruyat (2014).                |
| 730 | This intermediate element varies much in shape, but usually tapers anteriorly (e.g., MJSN                     |
| 731 | SCR011-140, MJSN SCR011-160, MJSN SCR011-276). In one specimen (MJSN TCH006-                                  |
| 732 | 1420; Figs. 8A-8B) the intermediate element is fused to the first suprapygal.                                 |
| 733 | Plesiochelys bigleri usually has two suprapygals that are clearly wider than long. Although                   |
| 734 | irregular in shape (usually from trapezoidal to sub-triangular), the first suprapygal usually tapers          |
| 735 | anteriorly and the second posteriorly (e.g., MJSN BSY009-815, MJSN SCR011-160, MJSN                           |
| 736 | TCH006-1420; Figs. 8A-8B). The two suprapygals can fuse into a single element (e.g., MJSN                     |
| 737 | TCH007-519, MJSN SCR011-148). In some specimens, the first suprapygal is divided in two                       |
| 738 | (e.g., MJSN SCR011-30, MJSN TCH007-252; Figs. 7A-7B). The pygal is a trapezoidal element                      |
| 739 | that is wider than long. Its relative size varies substantially from one individual to another.               |
| 740 |   |
| 741 | Costals and peripherals. Plesiochelys bigleri has eight costals and eleven peripherals. Their                 |
| 742 | shape and arrangement are relatively stable within the species. The length-width ratio of costal 4            |
| 743 | corresponds to that of Pl. etalloni and differs notably from that of Craspedochelys jaccardi                  |
|     |   |





(Anguetin, Püntener & Billon-Bruyat, 2014). The costals in *Pl. bigleri* are not as thick as the 744 same elements in *Pl. etalloni*. In the latter the proximal part of the costals is very thick, matching 745 the thick neural bones, and the costals usually remain relatively thick on their distal margin. In 746 Pl. bigleri, both the proximal and distal parts of the costals are thinner. A midline contact occurs 747 frequently between costals 7 (e.g., MJSN SCR011-140; Figs. 8I-8J), sometimes also between 748 749 costals 6 (e.g., MJSN SCR011-30, MJSN TCH006-1420; Figs. 8A–8B), and rarely between costals 8 (e.g., MJSN TCH005-42; Figs. 8M-8N). Such a reduction of posterior neurals and 750 midline contacts of costals can also occur in Pl. etalloni (e.g., MAJ 2005-11-1, MJSN TCH006-751 574), but more rarely than in *Pl. bigleri*. This condition appears to occur more commonly in 752 Craspedochelys jaccardi (Anguetin, Püntener & Billon-Bruyat, 2014). 753 754 Scutes of the carapace. There are three cervical scutes of about equal size in *Pl. bigleri* (best 755 preserved in MJSN CRT007-2 and MJSN TCH007-519). However, as common in plesiochelyids 756 (see Anguetin, Püntener & Billon-Bruyat, 2014), cervical scutes are difficult to discern in many 757 specimens. 758 There are usually five vertebrals, four pleurals, and twelve marginals. Vertebrals 1 and 5 759 760 are always the shortest in the series. The second and third vertebrals are rectangular (e.g., MJSN BSY009-815) to hexagonal (e.g., MJSN SCR011-30) in shape and cover one third (e.g., MJSN 761 762 TCH007-519) to about half (e.g., MJSN TCH006-767) of the costal length laterally. Vertebral 4 763 is usually hexagonal in shape. In some specimens it almost extends as far as the peripherals laterally, significantly reducing the size of pleural 4 (e.g., MJSN BSY006-326 and MJSN 764 765 SCR011-160). The intervertebral scute sulci usually run on neurals 1, 3, and 5. The scute sulcus 766 between vertebrals 4 and 5 most often runs on the intermediate element (e.g., MJSN BSY009-





| 767 | 815), but can also cross neural 8 (e.g., MJSN SCR011-148) or the first suprapygal (e.g., MJSN        |
|-----|--|
| 768 | TCH007-252; Fig. 7B). The twelfth pair of marginals is either restricted to the pygal and            |
| 769 | peripheral 11 (e.g., MJSN BSY006-326, MJSN TCH006-767), or extends on the second                     |
| 770 | suprapal (e.g., MJSN TCH006-1420, MJSN SCR011-140; Figs. 8B and 8J).                                 |
| 771 | One specimen (MJSN TCH005-42; Figs. 8M–8N) shows an anomalous scute pattern. It                      |
| 772 | has eight partially wedged vertebrals and five irregularly sized pleurals (maybe even six on the     |
| 773 | right side). This scute pattern shows no symmetry and we consider it as an anormal condition in      |
| 774 | Pl. bigleri.   |
| 775 |  |
| 776 | Plastron   |
| 777 |  |
| 778 | General description. Elements of the plastron are preserved in 40 out of the 41 shells herein        |
| 779 | referred to <i>Pl. bigleri</i> . With 481 mm, MJSN SCR10-1279 has the longest preserved plastron. In |
| 780 | contrast, the well preserved juvenile specimen MJSN SCR010-327 has a plastron length of only         |
|     |  |

194 mm. The anterior plastral lobe of *Pl. bigleri* is often somewhat quadrangular in outline (e.g., MJSN SCR010-1196, MJSN SCR011-140; Figs. 8K–8L), but can also be rounded (e.g., MJSN

CRT007-2), or even pointed (e.g., MJSN TCH006-1420; Figs. 8C–8D) in some specimens. In *Pl*.

etalloni, the anterior plastral lobe usually has a rather rounded, sometimes pointed, anterior

outline (Anquetin, Püntener & Billon-Bruyat, 2014). Like in Pl. etalloni, a central plastral

fontanelle (always longer than wide) is occasionally present (e.g., MJSN TCH006-1420; MJSN

787 BSY006-307; Figs. 8C-8D and 8G-8H).

788

783

784

785

786





Epiplastra and entoplastron. The shape of the epiplastra varies from rather rectangular (MJSN SCR010-1196) to triangular (e.g., MJSN TCH006-1420; Figs. 8C–8D). The anterolateral border of the epiplastra is often somewhat angular, mirroring the anterior outline of the anterior plastral lobe. Epiplastral bulbs, as described in *Pl. etalloni* (Bräm, 1965; Anquetin, Püntener & Billon-Bruyat, 2014), are absent or only weakly expressed (e.g., MJSN TCH007-252; Fig. 7C). The entoplastron is usually roundish (e.g., MJSN SCR011-140; Figs. 8K–8L) to roughly kite-shaped (e.g., MJSN TCH007-252; Figs. 7C–7D), but its relative size and length-width proportion varies greatly from one individual to another. The entoplastron of the juvenile specimen MJSN SCR010-327 is elongated and kite-shaped.

Hyo-, hypo-, and xiphiplastra. The hypoplastra are always longer than wide, although only by a small amount in a few individuals (e.g., MJSN BSY009-815). This corresponds to what is known in *Pl. etalloni* and many other turtles, and contrasts with the condition in *C. jaccardi*, where the hypoplastra are clearly wider than long (Anquetin, Püntener & Billon-Bruyat, 2014). The suture between the hyo- and hypoplastra is generally straight, but sometimes shows individual symmetric anteroposterior projections (e.g., MJSN CRT007-2, MJSN BSY006-307; Figs. 8G–8H). There is a small supernumerary bone between the hypoplastra of the juvenile specimen MJSN SCR010-327, but the sutures of this roundish bone are absent on the visceral side of the plastron. The posterolateral borders of the hypoplastra often project so as to articulate with the corresponding notches of the xiphiplastra (e.g., MJSN SCR011-413). The xiphiplastra are always longer than wide and often asymmetric. In most specimens, the xiphiplastra are relatively long elements, possibly more elongated in proportion than in *Pl. etalloni*. However, in some



individuals the xiphiplastra appear to be significantly reduced in length, but still longer than wide (e.g., MJSN BSY009-815).

Scutes of the plastron. The gular and extragular scute sulci are relatively shallow. In *Pl. etalloni*, the gular and extragular sulci are usually deeper, notably anteriorly, as a result of the presence of the epiplastral bulbs. As in *Pl. etalloni*, the gular scute is either restricted to the epiplastra (e.g., MJSN CRT007-2), or extends to the entoplastron (e.g., MJSN TCH007-252; Fig. 7D). In those specimens where the plastral midline sulcus is discernable, it is irregularly sinuous, sometimes creating small supernumerary scutes (e.g., MJSN SCR011-30). A similar condition is also known in *Pl. etalloni*.

Generally, the sulcus between the humeral and pectoral scutes is straight, while the sulcus between the pectoral and abdominal scutes is curving anteriorly. The sulcus between the femoral and anal scutes is usually restricted to the xiphiplastron, but extends to the hypoplastron in some specimens. In the latter case, the anal scutes may form a rectangular anterior projection on the hypoplastra (e.g., MJSN SCR011-30). A similar variability is present in *Pl. etalloni* (Anquetin, Püntener & Billon-Bruyat, 2014).

There are usually four pairs of inframarginal scutes. As in *Pl. etalloni*, the third one is generally the longest in the series. It covers the suture between hyo- and hypoplastron. The juvenile specimen MJSN SCR010-327 shows a variation of this pattern by having three inframarginal scutes on the left hypoplastron. It is however unclear whether this resulted in a total of five inframarginal scutes on the left side and whether this was also the case on the right side. The inframarginal scutes usually extend laterally on the peripherals. Occasionally some of



| 833 | them are restricted to plastral elements (e.g., MJSN CRT007-2, MJSN TCH006-767). This is                 |
|-----|--|
| 834 | also a condition known in <i>Pl. etalloni</i> (Anquetin, Püntener & Billon-Bruyat, 2014).                |
| 835 |  |
| 836 | Pectoral girdle  |
| 837 | Eight partially preserved scapulae are associated with shells of Pl. bigleri (MJSN BSY008-567,           |
| 838 | MJSN BSY009-815, MJSN SCR011-30, MJSN SCR011-148, MJSN TCH007-252, MJSN                                  |
| 839 | TCH007-519, MJSN TCH005-42; Fig. 10). The two scapulae of MJSN BSY008-567 are                            |
| 840 | attached to the visceral side of the plastron by sediment, approximately in situ and in contact          |
| 841 | with the humeri. The other six scapulae are disarticulated.  |
| 842 | The dorsally projecting scapular process and anteromedially projecting acromion process                  |
| 843 | are elliptic cylinders. The distal parts of these processes are missing in most specimens. Only the      |
| 844 | acromion process in the right scapula of MJSN BSY008-567 is probably complete. It measures               |
| 845 | 59 mm from its distal end to the notch between the scapular process and the coracoid. The two            |
| 846 | processes form a scapular angle of $102^{\circ}$ in MJSN TCH005-42 (Fig. 10), the only scapula of $Pl$ . |
| 847 | bigleri where this angle can be measured with confidence. None of the scapulae associated with           |
| 848 | Pl. bigleri provides clear information about the nature of the glenoid fossa or about the articular      |
| 849 | surface for the coracoid. As in other plesiochelyids, as well as thalassemydids and eurysternids,        |
| 850 | the glenoid neck is well developed.  |
| 851 | The posteromedially projecting coracoid itself is only partially preserved in MJSN                       |
| 852 | TCH005-42 (proximal part) and MJSN TCH007-519 (distal part, partially covered by bones and               |
| 853 | sediment). It is unclear whether the disarticulated coracoid of MJSN TCH005-42 belongs to the            |
| 854 | left (preserved) or right (unpreserved) scapula. The short diaphysis is irregularly cylindric in         |
| 855 | cross section. It broadens proximally where it articulates with the scapular neck. The distal end        |



of the bone is missing, but the broadening diaphysis indicates yet the beginning of the coracoid blade. The latter is partially observable in MJSN TCH007-519, where it forms a broad blade.

The scapula is also known in *Pl. etalloni* (NMS 8584, NMS 8731, NMS 9153 and NMB 435), as well as in *Thalassemys bruntrutana* and *Thalassemys hugii* (Püntener, Anquetin & Billon-Bruyat, 2015). The scapular angle of *Pl. bigleri* (see above) corresponds to the angle previously measured for *Pl. etalloni* in specimens from Solothurn and contrasts with the wider angles in *Th. bruntrutana* and *Th. hugii* (Püntener, Anquetin & Billon-Bruyat, 2015: table 1). The scapula of *Pl. etalloni* does not show any significant anatomical differences to the scapula of *Pl. bigleri*.

### Humerus

Four humeri are associated with shells of *Pl. bigleri* (the proximal parts of both humeri of MJSN BSY008-567 and MJSN TCH007-252 respectively). While both humeri of MJSN TCH007-252 (Fig. 11) are disarticulated, the humeri of MJSN BSY008-567 are attached to the visceral side of the plastron by sediment, approximately in situ and in contact with the scapulae.

The proximal articulation is a hemispherical head that projects dorsally with approximately 135° from the horizontal plane of the humerus (only measurable in the humeri of MJSN TCH007-252). The anteriorly expanding lateral process is the smaller one, as in most cryptodires (Gaffney, 1990). A strong deltopectoral crest projects ventrally from its lateral border (best visible in the left humerus of MJSN TCH007-252; Figs. 11F–11G). The larger, posteriorly expanding medial process is only slightly bulged ventrally, so that the intertubercular fossa is mainly defined by the deltopectoral crest. More distally, the narrowing diaphysis forms a waist almost circular in section.



The humerus is also partly known in *Pl. etalloni* (NMS 8584 and NMB 435) and *Tropidemys langii* (MJSN VTT006-253 and MJSN VTT010-17). The observed features of the humerus of *Pl. bigleri* correspond in all aspects to the humerus of *Pl. etalloni*. According to Püntener et al. (2014), the humerus of *Tr. langii* (MJSN VTT006-253) has a more expanded medial process and a broader and flatter diaphysis. However, a more recent discovery of a humerus of *Tr. langii* (MJSN VTT010-17) contradicts this statement and suggests that the observed features of MJSN VTT006-253 are probably due to postmortem flattening. On the base of the new material, the humerus of *Tr. langii* does not show significant anatomical differences to the humerus of *Pl. bigleri* and *Pl. etalloni*.

### Radius and Ulna

The radius and ulna are only known in the holotype specimen (MJSN TCH007-252; Figs. 12A–12H). The ulna can be confidently identified as a right ulna, but the radius is more poorly preserved and is only tentatively identified as a right one. The radius is a slim bone with a cylindric diaphysis of only 5 mm diameter at its narrowest point (Figs. 12A–12D). The bone is twisted, so that the proximal and distal heads stand perpendicular to each other. Although not completely preserved, it is clear that the distal expansion was broader and flatter than the proximal one, which is a common condition in turtles.

The ulna is strongly bent along the long axis due to postmortem deformation (Figs. 12F and 12H). It is clearly broader than the radius. The proximal head forms a moderately concave sigmoid notch, and the olecranon is poorly developed. Below the proximal head, the medial surface of the bone bears a well developed bicipital tubercle (Figs. 12E–12G). The diaphysis is





flat and 7 mm broad at its narrowest point. Towards the distal end, the bone remains flat and broadens up to 16 mm. The articulation for the carpals is not preserved.

Bräm (1965) briefly described one radius of *Pl. etalloni* (NMS 8731). Unfortunately, only a fragment of this radius has been preserved into the present day, leaving only Bräm's description as a reference. According to Bräm (1965), the distal expansion of the radius of *Pl. etalloni* is larger and more stoutly built than the proximal expansion.

Both ulnae of the same specimen (NMS 8731) are preserved. The distal expansion of these bones is quadrangular in shape. In contrast, this part is triangular shaped in *Pl. bigleri*. However, it is not clear whether this is a real anatomical difference or whether it is due to an insufficient preservation of MJSN TCH007-252.

## Pelvic girdle

Ten partially preserved pelves are associated with shells of *Pl. bigleri* (MJSN BSY006-307, MJSN BSY-147, MJSN BSY009-815, MJSN SCR010-30, MJSN SCR011-148, MJSN SCR011-413, MJSN TCH006-767, MJSN TCH006-1420, MJSN TCH007-252, MJSN TCH007-519). The following description is mainly based on the sub-complete pelvis of MJSN BSY006-307 that is still articulated in its original three dimensional shape, though it suffered minor postmortem deformation (Figs. 13). Right and left halves of the pelvis are still interconnected posteriorly by the ischium plate. The anterior midline connection of the pubes is not preserved. Although both acetabula are completely preserved on both sides of the pelvis, the ilium and pubis are much better preserved on the right side.

The acetabulum is a relatively deep and somewhat kidney-shaped cavity (Fig. 13). Its longer axis (about 35 mm long in MJSN BSY006-307) lies in the horizontal plane, its shorter



axis (about 20 mm) in the vertical plane. The three bones of the pelvis (ilium, pubis, ischium) form the acetabulum with their proximal parts. The sutures between these bones are best visible on the medial surface of the right acetabular region in MJSN BSY006-307.

The ilium extends posterodorsally (Fig. 13). Proximally, where it contributes to the acetabulum, its maximal width reaches 29 mm. More distally it narrows to form an irregularly oval, slightly twisted shaft (about 15 mm wide in MJSN BSY006-307). At the distal end, the ilium is flatter and expands in the anteroposterior direction. However, the posterodorsal iliac process and the anterodorsal articulation surface with the sacral rib are only very partially preserved in *Pl. bigleri* (MJSN TCH007-519 and MJSN SCR011-30 respectively).

The proximal part of the pubis extends anteroventrally approximately in the same axis as the ilium (Fig. 13). It narrows below the acetabulum, but the shaft remains much broader and flatter than the ilium shaft. Distally, the pubis divides into two parts: a ventrally orientated lateral pubic process and an anteriorly orientated part that normally forms the thyroid fenestra together with the ischium. The lateral pubic process is about 24 mm long in MJSN BSY006-307. At the distal end it has an oval articulation surface (only partially preserved in MJSN BSY006-307) that rested on the dorsal surface of the xiphiplastra. The anteromedial part of the pubis is broken in MJSN BSY006-307, and the shape of the thyroid fenestra remains unclear in *Pl. bigleri*.

The ischium extends posteroventrally, first narrowing into a short, circular shaft, then broadening again medially in order to form a broad plate that meets the other ischium medially. This ischial plate is concave dorsally. The contact between ischium and pubis at the anterior margin of this plate is not preserved in any specimen. The lateral ischial process is strong and extends posteriorly from the ischium. Due to postmortem deformation, the right process is strongly bent dorsally in MJSN BSY006-307. The posterior margin of the ischium, between the





965

966

967

968

969

lateral ischial process and the midline contact with the other ischium, forms a shallow 947 depression. The ventral surface of the ischial plate is generally convex. It bears a shallow V-948 shaped rugose area that points anteriorly. 949 The exceptional preservation of the pelvis of MJSN BSY006-307 is unique among 950 plesiochelyids. Bräm (1965) described the pelvis of *Pl. etalloni* (mainly based on NMS 8731) 951 952 and C. jaccardi (based on NMS 8713–8718), but this material is strongly fragmented and deformed. The observable features correspond fairly well with the pelvis of *Pl. bigleri*, namely 953 the general shape of the ilium (well visible in NMS 8731). Bräm (1965) concluded that there are 954 no significant differences between the pelvis of *Pl. etalloni* and *C. jaccardi*. 955 956 **Femur** 957 Three femora are associated with shells of *Pl. bigleri* (both of MJSN SCR010-1279 and one of 958 MJSN TCH005-21). The femur of MJSN TCH005-21 is strongly deformed and its proximal part 959 is badly damaged. Only the proximal head of the left femur of MJSN SCR010-1279 is preserved. 960 The right femur of MJSN SCR010-1279 is almost completely preserved, but most of the bone 961 surface is covered by encrustation. The following description is therefore mainly based on the 962 963 right femur of MJSN SCR010-1279 (Figs. 14A–14D).

The femur of *Pl. bigleri* is essentially a straight bone that is only slightly arched dorsally. The dorsally projecting proximal head and the ventrally projecting distal articulations give the left femur an elongated S-shape in posterior view (Fig. 14D). The right femur of MJSN SCR010-1279 is 134 mm long. The proximal head projects from the long axis of the femur at an angle of about 50° (Figs. 14B and 14D). It is hemispherical, but elongated along the long axis of the femur (about twice as long as wide), which is apparently more consistent with swimming than





| 970 | walking (Zug, 1971). This contrasts with the more roundish femoral head of <i>Tr. langii</i> (Püntener |
|-----|--|
| 971 | et al., 2014). In ventral view, the two trochanters form a deep, narrow, and V-shaped                  |
| 972 | intertrochanteric fossa (Fig. 14C). The posteriorly situated trochanter major is slightly shorter      |
| 973 | than the trochanter minor (anteriorly), but expands more prominently on the horizontal plane.          |
| 974 | Lateral ridges on both trochanters form a shallow V-shaped depression just distal to the               |
| 975 | intertrochanteric fossa, giving the latter a terraced appearance.                                      |
| 976 | The diaphysis is oval to circular in cross section. The bone is gradually broadening towards           |
| 977 | the distal end. The condyles are only slightly less expanded than the trochanters. The medial          |
| 978 | condyle is strongly arched and tappers proximally. The lateral condyle is not completely               |
| 979 | preserved, but it seems smaller and more roundish than the medial condyle. A deep fossa (about         |
| 980 | 6 mm deep) separates the two articulation surfaces from each other (Fig. 14C).                         |
| 981 | Within plesiochelyids, the femur is partly known in Pl. etalloni (NMS 8584 and MNS                     |
| 982 | 8731), C. jaccardi (NMS 8713–8718), and Tr. langii (MJSN VTT010-13). Based on this                     |
| 983 | incomplete material, the femur of Pl. bigleri, Pl. etalloni and C. jaccardi cannot be                  |
| 984 | differentiated. On the other hand, these species differ from Tr. langii, in which the trochanters      |
| 985 | expand more prominently along the horizontal plane and the intertrochanteric fossa is shallower,       |
| 986 | wider, and more rounded at its base (Püntener et al., 2014).   |
| 987 |  |
| 988 | Fibula   |
| 989 | Two left fibulae are associated with shells of Pl. bigleri (MJSN TCH005-21 and MJSN SCR010-            |
| 990 | 1279). The proximal third of the fibula of MJSN TCH005-21 is missing. The fibula of MJSN               |
| 991 | SCR010-1279 is complete (Figs. 14E-14H). It is 84 mm long, which corresponds to 63% of the             |
| 992 | femur length. Proximally, the fibula is only slightly expanded and has a small, hemispherical          |



articulation surface facing moderately ventrally. A swelling on the medial edge probably marks the attachement site of the proximal tibiofibular ligament (Figs. 14E–14G). The shaft is a rather flat, elliptic cylinder. At its narrowest point it has only one third of the width of the proximal expansion. Distally, the fibula is almost twice as expanded as proximally. Here the bone is slightly concave dorsally and has a somewhat triangular articulation surface facing moderately ventrally (Figs. 14E and 14G). The attachement site for the distal tibiofibular ligament is again marked by a swelling on the medial edge of the bone (Figs. 14E–14G).

The fibula is also partly known in *Pl. etalloni* (NMS 8584 and MNS 8731) and *C. jaccardi* (NMS 8713–8718). Based on this incomplete and deformed material, the fibula of *Pl. bigleri*, *Pl. etalloni* and *C. jaccardi* cannot be differentiated.

### Vertebral column

Two disarticulated cervical vertebrae are associated with shells of *Pl. bigleri*. The cervical vertebra of MJSN TCH005-21 is almost complete, but somewhat deformed (Fig. 15). The cervical vertebrae associated with MJSN SCR011-30 is more damaged and lacks three zygapophyses. The precise position of these two vertebrae in the cervical series is unclear. The centrum is moderately elongated and oval in cross section (slightly flattened dorsoventrally). There is a robust, but low ventral keel running all of the length of the centrum in MJSN TCH005-21 (Fig. 15D; not preserved in MJSN SCR011-30). The two known cervical vertebra are amphicoelous, with oval and slightly concave central articulations (Figs. 15B and 15E). The neural arch is moderately high (especially posteriorly) and the neural spine is reduced to a low longitudinal ridge (MJSN SCR011-30). The prezygapophyses and postzygapophyses are widely separated (Figs. 15A and 15D). The articular surface of the prezygapophyses is oriented dorsally





and slightly medially. The anterior margin of the neural arch forms a deep embayment between 1016 the prezygapophyses (Fig. 15A). The articular surface of the postzygapophyses faces ventrally 1017 and slightly laterally. A strong V-shaped ridge occurs on the dorsal surface of the 1018 postzygapophyses and defines a deep triangular fossa between the postzygapophyses (Figs. 15A 1019 and 15E). The transverse processes is poorly developed and is situated anteriorly along the 1020 1021 centrum (MJSN SCR011-30). Cervical vertebrae are known in *Pl. etalloni* (NMS 8584), *C. jaccardi* (NMS 8713–8718), 1022 and Th. hugii (NMS 8595–8609). The cervical vertebrae of Pl. etalloni and C. jaccardi are 1023 strongly deformed and broken. The few discernable features are consistent with what is known in 1024 Pl. bigleri. The cervical vertebrae of Th. hugii are much better preserved, even though they 1025 suffered strong lateral pressure. Taking postmortem deformation into account, these cervical 1026 vertebrae are also consistent with what is known in Pl. bigleri: moderately long amphicoelous 1027 centrum, robust but low ventral keel, moderately high neural arch (notably posteriorly), and 1028 1029 widely separated zygapophyses. Thoracic vertebrae can best be observed in the articulated specimens MJSN BSY007-147 1030 and MJSN TCH007-519, as well as in the disarticulated specimen MJSN SCR011-30. The best 1031 1032 preserved centra in these specimens are biconcave, smoothly rounded ventrally and without keel: e.g., 6th thoracic vertebra in MJSN BSY007-147, 7th thoracic vertebra in MJSN TCH007-519, 1033 and the disarticulated thoracic vertebrae (probably 9th and 10th) of MJSN SCR011-30. In 1034 1035 contrast, the best preserved thoracic centra of Pl. etalloni are keeled: e.g., 1st thoracic vertebra of NMS 8723, 4th thoracic vertebra of NMS 8731, and 5th thoracic vertebra of MJSN TCH006-1036 1037 574. Bräm (1965) already pointed out the keeled anterior thoracic centra of *Pl. etalloni* and *C.* 



*jaccardi*. However, it remains unclear whether this keel is also present on posterior thoracic centra of these species, and whether *Pl. bigleri* also had keeled anterior thoracic centra.

One sacral and two caudal vertebrae of MJSN SCR011-30 are preserved. The sacral vertebra is short, and has two narrow prezygapophyses and a small keel on the centrum. The centrum of one caudal vertebra bears a robust ventral keel, similar to the cervical vertebrae. Poor preservation prevents any conclusion on the type of central articulation in the caudal vertebrae.

A still articulated series of caudal vertebrae is preserved in specimen NMS 8584 referred to *Pl. etalloni*. As far as observable, their shape is consistent with what is known in *Pl. bigleri*. Bräm (1965) described their centra as procoelous. However, the state of preservation of these centra does not allow to confirm Bräm's observation.

### PLESIOCHELYS ETALLONI

Fifteen specimens from Porrentruy are referred to *Plesiochelys etalloni* (Table 1). They are all represented by elements of the carapace and most of them also by the plastron. The shells MJSN BSY007-205, MJSN TCH005-332, and MJSN TCH006-574 are still articulated, the latter being by far the best preserved specimen (Fig. 16). Non-shell post-cranial material is only poorly preserved. For example, small remains of the scapula and pelvis are associated with MJSN BSY003-347, but the poor preservation impedes any anatomical comparisons.

As mentioned above, *Pl. bigleri* and *Pl. etalloni* mostly differ in their cranial anatomy. However, some characteristics of the shell allow to tell the two species apart. The main characters we used for this study are the thickness of neural and costal bones, and the presence and development of the epiplastral bulbs. In *Pl. bigleri*, the epiplastral bulbs are reduced or absent (Fig. 7C), whereas they are usually well developed in *Pl. etalloni* (Figs. 16D–16E). The



neural and costal bones of *Pl. etalloni* are usually remarkable for their great relative thickness (Fig. 9D). Specimens of adult size regularly have neurals reaching 15 to 20 mm in thickness. Similarly sized specimens of *Pl. bigleri* usually have a neural thickness ranging between 11 and 14 mm. However, there is a great deal of variation in both species, and the difference between the two is less obvious in juvenile specimens. Neural (and costal) thickness alone is therefore not always sufficient to discriminante between the two species. In order to test whether differences in neural thickness are significant in the two species, we measured 43 specimens referred to *Pl. bigleri*, *Pl. etalloni*, or *Plesiochelys* sp. (see below).

The newly discovered shells of *Pl. etalloni* show about the same range of variation as previously described for this species (Anquetin, Püntener & Billon-Bruyat, 2014). MJSN TCH006-574 is however remarkable in its extremely reduced fourth pleurals, which are restricted to the peripheral bones due to the great posterolateral development of the fourth vertebral scute (Fig. 16B). The fourth pleurals are similarly reduced in some specimens from Solothurn, but they always occupy at least a small part of the costals (e.g., NMS 8514 and NMS 8517; Anquetin, Püntener & Billon-Bruyat, 2014: figs. 2, 8). In MJSN TCH006-574, the twelfth pair of marginal scutes is restricted to the pygal, which is a common variation in *Pl. bigleri* (see above), but is unknown in other specimens referred to *Pl. etalloni* (Anquetin, Püntener & Billon-Bruyat, 2014).

### NEURAL THICKNESS IN PLESIOCHELYS

The neural length and thickness was measured on selected specimens (see Material and Methods; Fig. 17B; Table 3). The scatter plot of mean length and thickness measurements reveals a relatively clear separation between *Plesiochelys bigleri* and *Plesiochelys etalloni* (Fig. 17A).



This separation is mostly due to the proportionally increased neural thickness observed in Pl. etalloni, as confirmed by the Mann-Whitney tests for mean thickness and length/thickness ratio (p < 0.0001, respectively). Mean neural length however is not significantly different in the two species (p = 0.1156; Fig. 17D).

The discriminant analysis resulted in a relatively good classification of specimens (93.94% of individuals correctly identified; Fig. 17C). Only two specimens (MJSN BSY009-815 and MJSN TCH006-767) are incorrectly classified as *Pl. etalloni*. These two specimens happen to be the ones that lie the closest to the *Pl. etalloni* morphospace (Fig. 17A). The discriminant analysis also provided tentative classifications for the 10 indeterminate specimens (*Plesiochelys* sp.), which correspond fairly well with the conclusions we can draw based on the length/thickness scatter plot (Fig. 17A; Table 4). We consider the classification of only two of these indeterminate specimens to be dubious. MJSN BSY 009-310 is classified by the discriminant analysis as *Pl. etalloni*, but this specimen actually lies on the margin of the *Pl. bigleri* morphospace (Fig. 17A). SCR010-479 is classified by the discriminant analysis as *Pl. bigleri*, but lies so far from the known morphospaces of *Pl. bigleri* and *Pl. etalloni* that this classification must be regarded with caution for the moment.

Neural thickness is therefore a good character to help differentiating between *Pl. bigleri* and *Pl. etalloni*. In the analyzed sample, mean neural thickness ranges from 9.61 to 13.77 mm (mean = 11.95 mm) in *Pl. bigleri*, and from 12.82 to 17.76 mm (mean = 14.83 mm) in *Pl. etalloni* (Fig. 17E). This difference between the two species is even more clearly expressed in the length/thickness ratio, which ranges from 4 to 5.65 (mean = 4.79) in *Pl. bigleri*, and from 3.1 to 3.91 (mean = 3.67) in *Pl. etalloni* (Fig. 17F).



### **DISCUSSION**

## Alpha taxonomy

There is a dual issue with the identification and distinction of *Plesiochelys bigleri* and *Plesiochelys etalloni*. First, the two species are so closely related that differences in their shell and appendicular anatomy are minimal (see above). Second, each of the two species is known by tenths of shells from a single locality and horizon. These extensive collections reveal a great intraspecific variability in the two species (Anquetin, Püntener & Billon-Bruyat, 2014; this study). Therefore, differentiating the two species can be challenging.

The holotype (MJSN TCH007-252) and paratype (MJSN TCH006-1451) specimens of *Pl. bigleri* are of paramount importance to establish the distinction between the two species. The isolated cranium MJSN TCH006-1451 (Figs. 5 and 6) exhibits a number of characteristics that clearly set it apart from *Pl. etalloni*: reduced processus trochlearis oticum, reduced posterior flooring of the cavum acustico-jugulare by the pterygoid, clear prootic-opisthotic contact on the floor of the fossa temporalis superior, pila prootica not ossified, processus paroccipitalis extending posterolaterally, anterior foramen nervi abducentis opening ventral and slightly anteromedial to the base of the processus clinoideus, surface below the dorsum sellae sloping more gently anteriorly, and foramina anterius canalis carotici cerebralis widely separated. The preservation of the cranium associated with the holotype specimen (Fig. 4) is not as good as that of the paratype, but it also exhibits most of the above differences with *Pl. etalloni*, in addition to the following: more rounded foramen nervi trigemini, and absence of midline contact of the exoccipital in the floor of the foramen magnum. Most importantly, the cranium of the holotype is associated with a near-complete carapace and partial plastron (Fig. 7). The cranium was found



literally within the associated shell during preparation alongside elements of the appendicular skeleton. There is therefore no doubt regarding the natural state of this association. Interestingly, the holotype shell is remarkably similar to that of *Pl. etalloni*, except for the much thinner neural and costal bones and for the absence of epiplastral bulbs.

Among the 80 relatively complete shells studied herein, 41 can be confidently referred to the new species *Pl. bigleri* based on the reduced neural and costal thickness, the absence or great reduction of epiplastral bulbs, and a generally more quadrangular anterior plastral lobe. Among the remaining 39 shells, 15 exhibit features that are consistent with an identification as *Pl. etalloni*, notably the great thickness of neural and costal bones and/or the presence of well-developed epiplastral bulbs. The remaining 24 shells are provisionally identified as *Plesiochelys* sp. because they lack sufficient diagnostic features. Among the 56 specimens referred either to *Pl. bigleri* or to *Pl. etalloni*, 33 with well-preserved neural bones were selected for a statistical analysis of neural thickness. This analysis confirmed that the mean thickness and length/thickness ratio were statistically different in the two species, with a mean length/thickness ratio of 4.79 for *Pl. bigleri* and 3.67 for *Pl. etalloni* (see above). The length/thickness ratio of neural bones (notably from neurals 2 to 5) is therefore an important additional feature to consider in order to differentiate these two species.

## Is Plesiochelys bigleri also present in Solothurn?

The Solothurn turtle assemblage is diversified and slightly younger than the one from Porrentruy. However, the two localities share a number of species in common: *Plesiochelys etalloni*, *Tropidemys langii*, *Thalassemys hugii*, and *Thalassemys bruntrutana* (Rütimeyer, 1873; Bräm,

1965; Püntener et al., 2014; Püntener, Anquetin & Billon Bruyat, 2015). Given the similarity



1154

1155

1156

1157

1158

1159

1160

1161

1162

1163

1164

1165

1166

1167

1168

1169

1170

1171

1172

1173

observed between *Pl. bigleri* and *Pl. etalloni* in Porrentruy, the presence of *Pl. bigleri* among Solothurn specimens referred to *Pl. etalloni* would certainly not come as a surprise.

Six skulls from Solothurn are referred to *Pl. etalloni* (NMS 8738, NMS 8739, NMS 8740, NMS 9145, NMS 40870, and NMS 40871; Gaffney, 1975a; Gaffney, 1976; Anguetin, Püntener & Billon-Bruyat, 2015). They all appear to belong to that species, although there may be some doubts regarding NMS 9145 which is associated with unprepared postcranial material including relatively thin costal bones. Remaining specimens referred to *Pl. etalloni* are otherwise often preserved as articulated shells, which complicates observation of neural and costal bones thickness in some cases and prevents a statistical analysis of neural bone thickness. Most of these specimens exhibit traits that are compatible with *Pl. etalloni*, notably: relatively thick neurals or costal bones (e.g., NMS 8461, NMS 8515, NMS 8517, NMS 8732), well-developed epiplastral bulbs (e.g., NMS 8533, NMS 8693, NMS 9150, NMS 9153, NMS 9173), or both features at the same time (e.g., NMS 8582). In some specimens, neither of the two main distinguishing features can be observed due to preservation (e.g., NMS 8727). The attribution of other specimens might be questioned because one of the distinguishing feature is poorly expressed, whereas the other is impossible to check. For example, NMS 8731 has only moderately expressed epiplastral bulbs, and the thickness of the neurals and costals is difficult to evaluate (the costals seem to be relatively thin).

For the moment, none of the *Plesiochelys* specimens from Solothurn can be confidently referred to *Pl. bigleri*. However, this material should definitely be re-evaluated in the future in light of the new material from Porrentruy.

1174

1175

### **CONCLUSIONS**





Plesiochelys bigleri is a new plesiochelyid turtle known based on 41 relatively complete, but mostly disarticulated shells and two crania (one associated with a shell, and another one isolated). All of this material originates from a series of close by localities west of the small town of Courtedoux, near Porrentruy, Canton of Jura, Switzerland. Most of the specimens were collected from a single stratigraphically limited horizon, the Lower Virgula Marls, dated from the early late Kimmeridgian. A few additional specimens were found in two underlying horizons, the Corbis Limestones and Banné Marls, dated from the late early Kimmeridgian.

The shell morphology of *Pl. bigleri* is remarkably similar to that of *Pl. etalloni*, a species known based on tenths of shells and several crania from the Kimmeridgian of Switzerland, France, Germany, and England. These two closely related species however differ in the thickness of the neural and costal bones of the carapace (a difference that is statistically tested herein), and the presence and development of the epiplastral bulbs in the plastron. Differentiating the two species based only on shell morphology can be challenging in some incomplete or juvenile individuals. The two species co-occur in Porrentruy and 24 shells (30% of the shells referable to *Plesiochelys*) cannot be identified at the species level as a result of this great similarity. However, the two species are more easily separated based on cranial morphology. Actually, *Pl. bigleri* exhibits cranial features that clearly set it apart from *Pl. etalloni* and other plesiochelyids, such as: a rounded foramen nervi trigemini, a shallow pterygoid fossa, a reduced processus trochlearis oticum, the absence of ossification of the pila prootica, the surface below the dorsum sellae sloping rather gently anteroventrally, and the widely separated foramina anterius canalis carotici cerebralis.

For the moment, *Pl. bigleri* is known only in Porrentruy. However, Solothurn and Porrentruy share several species of turtles in common (*Pl. etalloni*, *Tropidemys langii*,



| 1199 | Thalassemys            | hugii, and Thalassemys bruntrutana), and these species are also known in the        |
|------|------------------------|---|
| 1200 | Kimmeridgia            | an of southern England (Püntener et al., 2014; Püntener, Anquetin & Billon-Bruyat,  |
| 1201 | 2015; Anque            | tin & Chapman, 2016). Finding Pl. bigleri in other localities would therefore not   |
| 1202 | come as a sur          | rprise.   |
| 1203 | The ab                 | undant material from Solothurn and Porrentruy referred to Pl. etalloni and Pl.      |
| 1204 | <i>bigleri</i> illustr | rates the extent of intraspecific variability in these two species. Although these  |
| 1205 | results may r          | not be blindly transposable to other groups of turtles, they represent an important |
| 1206 | point of com           | parison for other studies on Mesozoic turtle diversity.                             |
| 1207 |                        |   |
| 1208 | Institutional          | Abbreviations   |
| 1209 | MAJ                    | Musée d'archéologie du Jura, Lons-le-Saunier, France                                |
| 1210 | MJSN                   | JURASSICA Museum, Porrentruy, Switzerland   |
| 1211 | NHMUK                  | Natural History Museum, London, UK  |
| 1212 | NMB                    | Naturhistorisches Museum Basel, Switzerland   |
| 1213 | NMS                    | Naturmuseum Solothurn, Switzerland  |
| 1214 | OUMNH                  | Oxford University Museum of Natural History, Oxford, UK                             |
| 1215 | PIMUZ                  | Paläontologisches Institut und Museum, Universität Zürich, Switzerland              |
| 1216 |                        |   |
| 1217 | Locality Ab            | breviations   |
| 1218 | BSY                    | Bois de Sylleux, Courtedoux, near Porrentruy, Switzerland                           |
| 1219 | CRT                    | Crat, Chevenez, near Porrentruy, Switzerland  |
| 1220 | SCR                    | Sur Combe Ronde, Courtedoux, near Porrentruy, Switzerland                           |
| 1221 | ТСН                    | Tchâfoué, Courtedoux, near Porrentruy, Switzerland                                  |



| 1222 | VTT  | Vâ Tche Tchâ, Courtedoux, near Porrentruy, Switzerland                                       |
|------|--|--|
| 1223 |  |  |
| 1224 | ACKNOWL  | EDGEMENTS  |
| 1225 | We thank Loï   | c Bocat (excavation), Pierre Bigler, Renaud Roch and Sébastien Bergot                        |
| 1226 | (preparation t   | eam), Bernard Migy and Olivier Noaillon (photographs), Pierre Widder (scientific             |
| 1227 | drawings), Ap  | polline Lefort (discussion on stratigraphy) and the whole Paleontology A16 team.             |
| 1228 | We furthermore thank Silvan Thüring (NMS) and Loïc Costeur (NMB) for access to collections |  |
| 1229 | in their care.   |  |
| 1230 |  |  |
| 1231 | REFERENC   | ES   |
| 1232 | Anquetin J, C  | hapman SD. 2016. First report of Plesiochelys etalloni and Tropidemys langii from            |
| 1233 | the La   | te Jurassic of the UK and the palaeobiogeography of plesiochelyid turtles. Royal             |
| 1234 | Societ   | y Open Science 3:150470. DOI: 10.1098/rsos.150470.   |
| 1235 | Anquetin J, D  | beschamps S, Claude J. 2014. The rediscovery and redescription of the holotype of            |
| 1236 | the La   | te Jurassic turtle <i>Plesiochelys etalloni</i> . <i>PeerJ</i> 2:e258 DOI 10.7717/peerj.258. |
| 1237 | Anquetin J, P  | üntener C, Billon-Bruyat J-P. 2014. A taxonomic review of the Late Jurassic                  |
| 1238 | eucryp   | otodiran turtles from the Jura Mountains (Switzerland and France). <i>PeerJ</i> 2:e369.      |
| 1239 | DOI:   | 10.7717/peerj.369.   |
| 1240 | Anquetin J, P  | üntener C, Billon-Bruyat J-P. 2015. Portlandemys gracilis n. sp., a new coastal              |
| 1241 | marin  | e turtle from the Late Jurassic of Porrentruy (Switzerland) and a reconsideration of         |
| 1242 | plesio   | chelyid cranial anatomy. <i>PLOS ONE</i> 10:e0129193. DOI:                                   |
| 1243 | 10.137   | 71/journal.pone.0129193.   |
|      |  |  |



| 1244 | Bardet N. 1994. Extinction events among Mesozoic marine reptiles. <i>Historical Biology</i> 7:313– |
|------|--|
| 1245 | 324.   |
| 1246 | Bardet N. 1995. Evolution et extinction des reptiles marins au cours du Mésozoïque.                |
| 1247 | Palaeovertebrata 24:177–283.   |
| 1248 | Bardet N, Falconnet J, Fischer V, Houssaye A, Jouve S, Pereda Suberbiola X, Pérez-García A,        |
| 1249 | Rage J-C, Vincent P. 2014. Mesozoic marine reptile palaeobiogeography in response to               |
| 1250 | drifting plates. Gondwana Research 26:869-887. DOI: 10.1016/j.gr.2014.05.005.                      |
| 1251 | Batsch AJGC. 1788. Versuch einer Anleitung, zur Kenntniß und Geschichte der Thiere und             |
| 1252 | Mineralien. Jena: Akademische Buchhandlung.  |
| 1253 | Baur G. 1888. Osteologische Notizen über Reptilien (Fortsetzung II). Zoologischer Anzeiger         |
| 1254 | 11:417–424.  |
| 1255 | Billon-Bruyat J-P. 2005a. A "turtle cemetery" from the Late Jurassic of Switzerland. Abstracts,    |
| 1256 | 3rd Swiss Geoscience Meeting, Zürich: 238.   |
| 1257 | Billon-Bruyat J-P. 2005b. First record of a non-pterodactyloid pterosaur (Reptilia: Archosauria)   |
| 1258 | from Switzerland. Eclogae Geologicae Helvetiae 98:313-317.   |
| 1259 | Billon-Bruyat J-P, Marty D, Bocat L, Paratte G. 2012. Under the feet of sauropods: a trampled      |
| 1260 | coastal marine turtle. Abstracts, Symposium on turtle evolution, Tübingen: 10.                     |
| 1261 | Bräm H. 1965. Die Schildkröten aus dem oberen Jura (Malm) der Gegend von Solothurn.                |
| 1262 | Schweizerische Paläontologische Abhandlungen 83:1–190.   |
| 1263 | Comment G, Ayer J, Becker D. 2011. Deux nouveaux membres lithostratigraphiques de la               |
| 1264 | Formation de Reuchenette (Kimméridgien, Ajoie, Jura suisse) - Nouvelles données                    |
| 1265 | géologiques et paléontologiques acquises dans le cadres de la construction de l'autoroute          |
| 1266 | A16 (Transjurane). Swiss Bulletin für angewandte Geologie 16:3–24.                                 |
|      |  |



| 1267 | Comment G, Lefort A, Koppka J, Hantzpergue P. 2013. Le Kimmentigien d'Ajoie (Jura, Suisse).                   |
|------|---|
| 1268 | lithostratigraphie et biostratigraphie de la Formation de Reuchenette. Revue de                               |
| 1269 | Paléobiologie 34:161–194. DOI: 10.5281/zenodo.34341.  |
| 1270 | Dollo L. 1886. Première note sur les Chéloniens du Bruxellien (Eocène moyen) de la Belgique.                  |
| 1271 | Bulletin du Musée Royal d'Histoire Naturelle de Belgique 4:75–100.  |
| 1272 | Gaffney ES. 1972. An illustrated glossary of turtle skull nomenclature. American Museum                       |
| 1273 | Novitates 2486:1–33.  |
| 1274 | Gaffney ES. 1975a. A taxonomic revision of the Jurassic turtles <i>Portlandemys</i> and <i>Plesiochelys</i> . |
| 1275 | American Museum Novitates 2574:1–19.  |
| 1276 | Gaffney ES. 1975b. Solnhofia parsonsi, a new cryptodiran turtle from the Late Jurassic of                     |
| 1277 | Europe. American Museum Novitates 2576:1–22.  |
| 1278 | Gaffney ES. 1975c. A phylogeny and classification of the higher categories of turtles. Bulletin of            |
| 1279 | the American Museum of Natural History 155:387–436.   |
| 1280 | Gaffney ES. 1976. Cranial morphology of the European Jurassic turtles <i>Portlandemys</i> and                 |
| 1281 | Plesiochelys. Bulletin of the American Museum of Natural History 157:487–544.                                 |
| 1282 | Gaffney ES. 1979. Comparative cranial morphology of Recent and fossil turtles. Bulletin of the                |
| 1283 | American Museum of Natural History 164:65–376.  |
| 1284 | Gaffney ES. 1990. The comparative osteology of the Triassic turtle <i>Proganochelys</i> . Bulletin of         |
| 1285 | the American Museum of Natural History 194:1–263.   |
| 1286 | Hammer Ø, Harper DAT, Ryan PD. 2001. PAST: Paleontological statistics software package for                    |
| 1287 | education and data analysis. Palaeontologia Electronica 4(9).   |
|      |   |



| 1288 | Joyce WG, Parham JF, Gauthier JA. 2004. Developing a protocol for the conversion of rank-        |
|------|--|
| 1289 | based taxon names to phylogenetically defined clade names, as exemplified by turtles.            |
| 1290 | Journal of Paleontology 78:989–1013.   |
| 1291 | Karl H-V, Staesche U, Tichy G, Lehmann J, Peitz S. 2007. Systematik der Schildkröten             |
| 1292 | (Anapsida: Chelonii) aus Oberjura und Unterkreide von Nordwestdeutschland.                       |
| 1293 | Geologisches Jahrbuch B 98:5–89.   |
| 1294 | Koppka J. 2015. Revision of the Bivalvia from the Upper Jurassic Reuchenette Formation,          |
| 1295 | Northwest Switzerland—Ostreoidea. Zootaxa 3927(1):1–117.   |
| 1296 | Leuzinger L, Kocsis L, Billon-Bruyat J-P, Spezzaferri S, Vennemann T. 2015. Stable isotope       |
| 1297 | study of a new chondrichthyan fauna (Kimmeridgian, Porrentruy, Swiss Jura): an unusual           |
| 1298 | freshwater-influenced isotopic composition for the hybodont shark Asteracanthus.                 |
| 1299 | Biogeosciences 12:6945–6954.   |
| 1300 | Maack GA. 1869. Die bis jetzt bekannten fossilen Schildkröten und die im oberen Jura bei         |
| 1301 | Kelheim (Bayern) und Hannover neu aufgefundenen ältesten Arten derselben.                        |
| 1302 | Palaeontographica 18:193–338.  |
| 1303 | Mallison H, Wings O. 2014. Photogrammetry in paleontology – A practical guide. <i>Journal of</i> |
| 1304 | Paleontological Techniques 12:1–30.  |
| 1305 | Marty D. 2008. Sedimentology, taphonomy, and ichnology of Late Jurassic dinosaur tracks from     |
| 1306 | the Jura carbonate platform (Chevenez-CombeRonde tracksite, NW Switzerland):                     |
| 1307 | insights into the tidalflat palaeoenvironment and dinosaur diversity, locomotion, and            |
| 1308 | palaeoecology. GeoFocus 21:1–278.  |
|      |  |



| 1309 | Marty D, Hug WA. 2003. Le Kimmeridgien en Ajoie (Mesozoique): premiers resultats de                  |
|------|--|
| 1310 | fouilles et de recherches paléontologique sur le tracé de la Transjurane (A16). Actes de la          |
| 1311 | Société jurassienne d'émulation 2003:27–44.  |
| 1312 | Marty D, Billon-Bruyat J-P. 2009. Field-trip to the excavations in the Late Jurassic along the       |
| 1313 | future Transjurane highway near Porrentruy (Canton Jura, NW Switzerland): dinosaur                   |
| 1314 | tracks, marine vertebrates and invertebrates [Abstract]. In: Billon-Bruyat J-P, Marty D,             |
| 1315 | Costeur L, Meyer CA, Thüring B, eds. Abstracts and Field Guides, 5th International                   |
| 1316 | Symposium on Lithographic Limestone and Plattenkalk, Actes 2009 bis de la Société                    |
| 1317 | jurassienne d'émulation. Porrentruy, Switzerland, 94-129.  |
| 1318 | Marty D, Ayer J, Becker D, Berger J-P, Billon-Bruyat J-P, Braillard L, Hug WA, Meyer CA.             |
| 1319 | 2007. Late Jurassic dinosaur tracksites of the Transjurane highway (Canton Jura, NW                  |
| 1320 | Switzerland): overview and measures for their protection and valorization. Bulletin for              |
| 1321 | Applied Geology 12:75–89.  |
| 1322 | Meyer CA. 1994. Depositional environment and paleoecology of the Solothurn turtle limestone          |
| 1323 | (Kimmeridgian, Northern Switzerland). Geobios 27 (Supplement 1):227-236.                             |
| 1324 | Meyer H von. 1864. Parachelys Eichstättensis aus dem lithographischen Schiefer von Eichstätt.        |
| 1325 | Palaeontographica 11:289–295.  |
| 1326 | Oertel W. 1924. Die Schildkrötenfauna des nordwestdeutschen oberen Jura. Paläontologische            |
| 1327 | Zeitschrift 6:43–79.   |
| 1328 | Owen R. 1842. Report on British fossil reptiles, part II. Report for the British Association for the |
| 1329 | Advancement of Science, Plymouth 1841 11:60–204.   |
| 1330 | Parsons TS, Williams EE. 1961. Two Jurassic turtle skulls: A morphological study. Bulletin of        |
| 1331 | the Museum of Comparative Zoology 125:43–107.  |



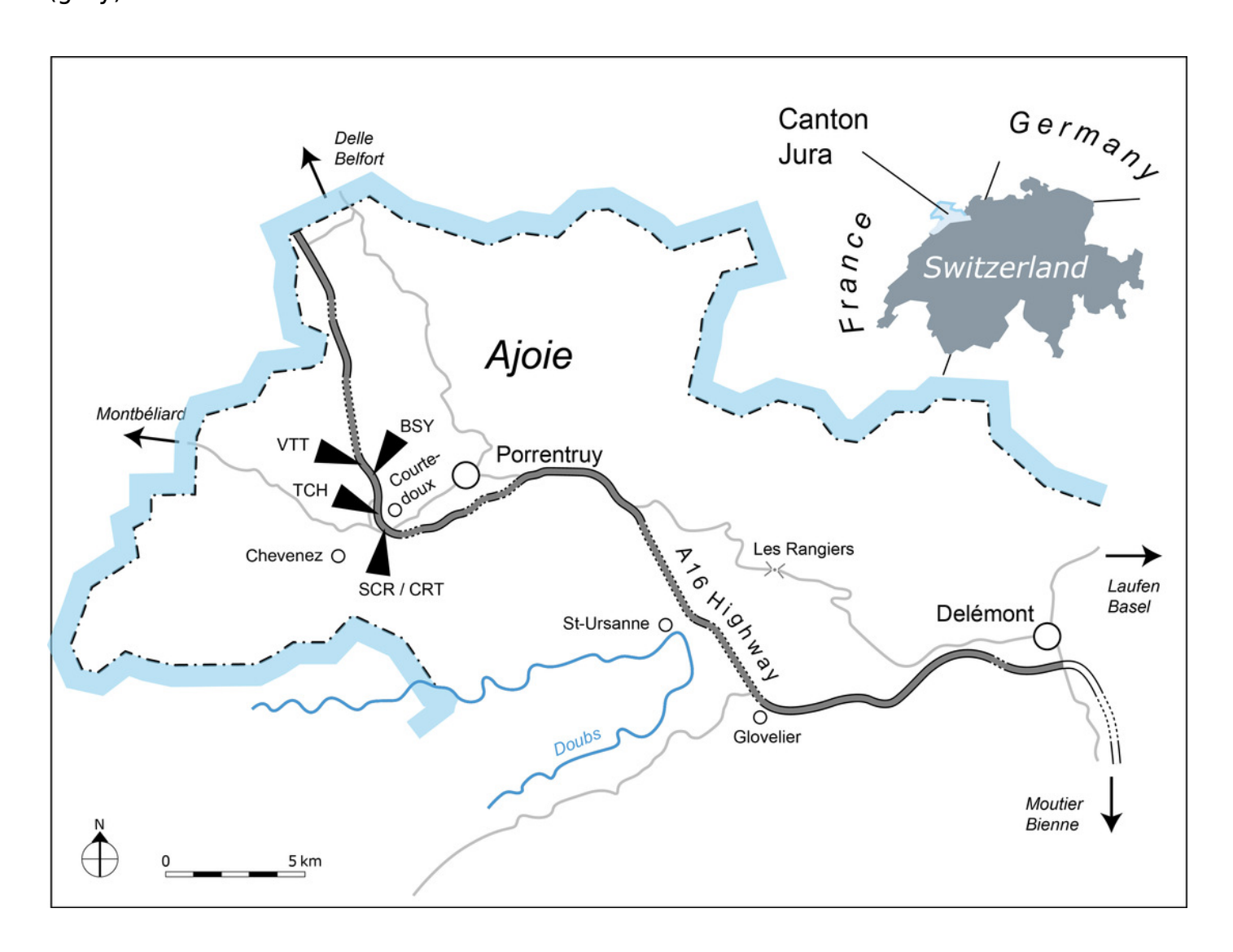
| 1332 | Perez-Garcia A. 2015. New data on the poorly-known Late Jurassic turtles <i>Indiassemys</i> and       |
|------|---|
| 1333 | Enaliochelys and description of a new basal eucryptodiran taxon. Journal of Iberian                   |
| 1334 | Geology 41:21–30. DOI: 10.5209/rev_JIGE.2015.v41.n1.48652.  |
| 1335 | Pérez-García A, Scheyer TM, Murelaga X. 2013. The turtles from the Uppermost Jurassic and             |
| 1336 | Early Cretaceous of Galve (Iberian Range, Spain): anatomical, systematic,                             |
| 1337 | biostratigraphic and palaeobiogeographical implications. Cretaceous Research 44:64-82.                |
| 1338 | Pérez-García A, Ortega F, Murelaga X, Dantas P. 2008. Plesiochelys sp. (Testudines;                   |
| 1339 | Eucryptodira) de la Fm. Freixial (Jurásico Superior) en Ulsa (Torres Vedras, Portugal).               |
| 1340 | Publicaciones del Seminario de Paleontología de Zaragoza 8:331–344.                                   |
| 1341 | Philippe M, Billon-Bruyat J-P, Garcia-Ramos JC, Bocat L, Gomez B, Piñuela L. 2010. New                |
| 1342 | occurrences of the wood Protocupressinoxylon purbeckensis Francis: implications for                   |
| 1343 | terrestrial biomes in southwestern Europe at the Jurassic/Cretaceous boundary.                        |
| 1344 | Palaeontology 53:201–214.   |
| 1345 | Pictet F-J, Humbert A. 1857. Description d'une émyde nouvelle ( <i>Emys Etalloni</i> ) du terrain     |
| 1346 | jurassique supérieur des environs de St-Claude. In: Pictet F-J, ed. Matériaux pour la                 |
| 1347 | paléontologie suisse, Première série. Genève: J. Kessmann, 1–10.                                      |
| 1348 | Püntener C, Billon-Bruyat J-P, Bocat L, Berger J-P, Joyce WG. 2014. Taxonomy and phylogeny            |
| 1349 | of the turtle Tropidemys langii Rütimeyer, 1873 based on new specimens from the                       |
| 1350 | Kimmeridgian of the Swiss Jura Mountains. Journal of Vertebrate Paleontology 34:353-                  |
| 1351 | 374. DOI: 10.1080/02724634.2013.804412.   |
| 1352 | Püntener C, Anquetin J, Billon-Bruyat J-P. 2015. <i>Thalassemys bruntrutana</i> n. sp., a new coastal |
| 1353 | marine turtle from the Late Jurassic of Porrentruy (Switzerland), and the                             |
| 1354 | paleobiogeography of the Thalassemydidae. <i>PeerJ</i> 3:e1282. DOI: 10.7717/peerj.1282.              |



| 1355 | Rabi M, Zhou C-F, Wings O, Ge S, Joyce WG. 2013. A new xinjiangchelyid turtle from the            |
|------|---|
| 1356 | Middle Jurassic of Xinjiang, China and the evolution of the basipterygoid process in              |
| 1357 | Mesozoic turtles. BMC Evolutionary Biology 13:203.  |
| 1358 | Rieppel O. 1980. The skull of the Upper Jurassic cryptodire turtle <i>Thalassemys</i> , with a    |
| 1359 | reconsideration of the chelonian braincase. <i>Palaeontographica</i> , <i>Abt. A</i> 171:105–140. |
| 1360 | Rütimeyer L. 1873. Die fossilen Schildkröten von Solothurn und der übrigen Juraformation.         |
| 1361 | Neue Denkschrift der allgemeinen schweizerischen naturforschenden Gesellschaft 25:1-              |
| 1362 | 185.  |
| 1363 | Schaefer K. 2012. Variabilité de la morphologie dentaire des crocodiliens marins                  |
| 1364 | (Thalattosuchia) du Kimméridgien d'Ajoie (Jura, Suisse). Unpublished Master Thesis,               |
| 1365 | University of Fribourg.   |
| 1366 | Werneburg I. 2011. The cranial musculature of turtles. <i>Palaeontologia Electronica</i> 14:15A.  |
| 1367 | Zangerl R. 1969. The turtle shell. In: Gans C, Bellairs AA, Parsons TS, eds. Biology of the       |
| 1368 | Reptilia. Volume 1, Morphology A. London: Academic Press, 311–339.                                |
| 1369 | Zittel KA. 1889. Handbuch der Palaeontologie. Section 1: Palaeozoologie, Volume 3,                |
| 1370 | Vertebrata, Shipment 3: Reptilia. München: R. Oldenbourg.   |
| 1371 | Zug GR. 1971. Buoyancy, locomotion, morphology of the pelvic girdle and hindlimb, and             |
| 1372 | systematics of cryptodiran turtles. Miscellaneous Publications Museum of Zoology,                 |
| 1373 | University of Michigan 142:1–98.  |
|      |   |

Geographical map of the Ajoie Region, Canton Jura, Switzerland.

The five excavation sites Bois de Sylleux (BSY), Crat (CRT), Sur Combe Ronde (SCR), Tchâfouè (TCH), and Vâ Tche Tchâ (VTT) are situated along the Transjurane A16 highway (gray).

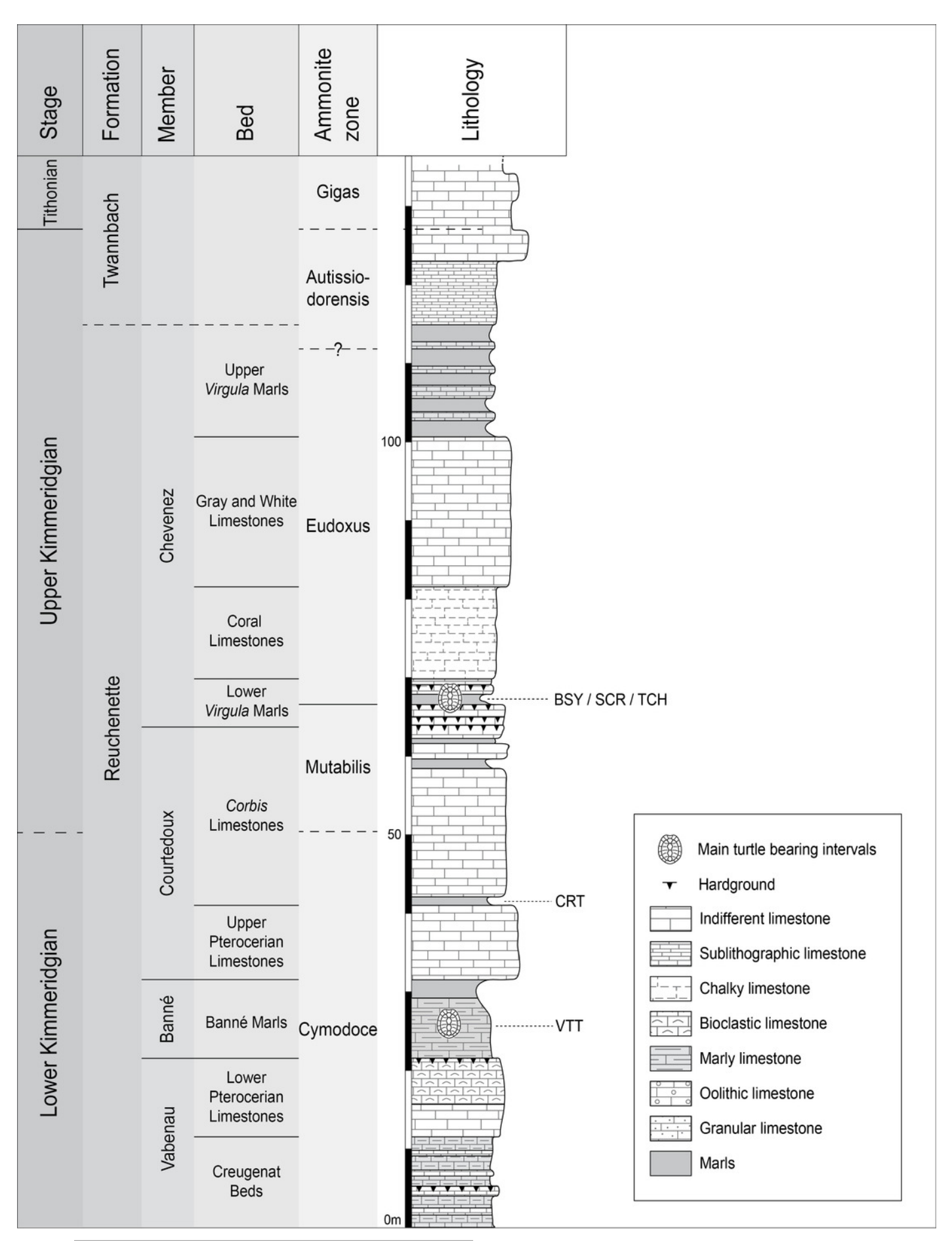




Stratigraphic section of the Reuchenette Formation.

Most specimens were discovered within the Lower *Virgula* Marls (sites of BSY, SCR, and TCH). One specimen comes from dinosaur track-bearing tidal laminites (CRT), and two from the Banné Marls (VTT). Scheme modified after Comment et al. (2015).





MJSN TCH006-1420, Plesiochelys bigleri (Kimmeridgian, Porrentruy, Switzerland).

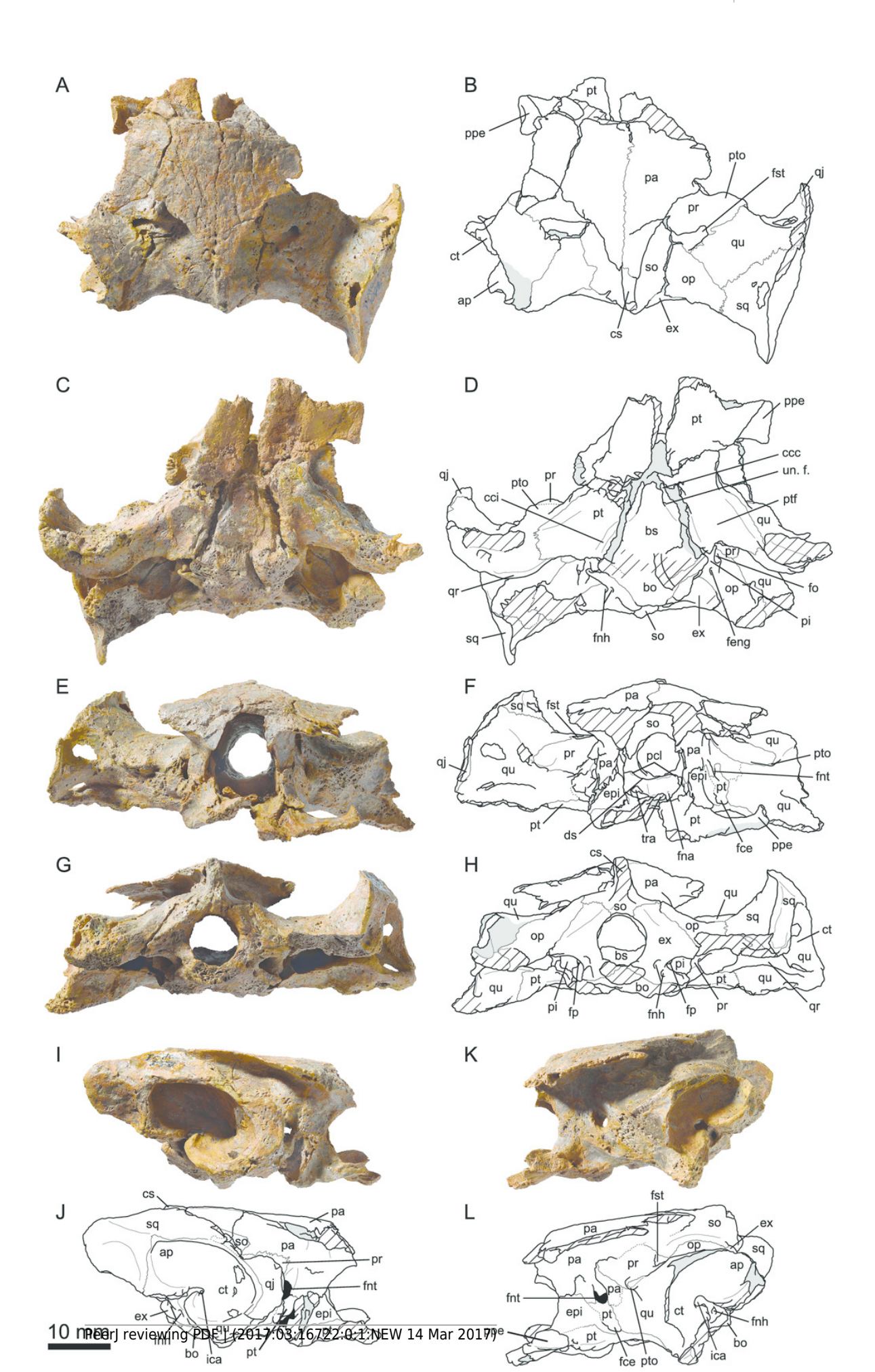
Field photograph of the specimen embedded in the Lower Virgula Marls.





MJSN TCH007-252, holotype of *Plesiochelys bigleri* (Kimmeridgian, Porrentruy, Switzerland).

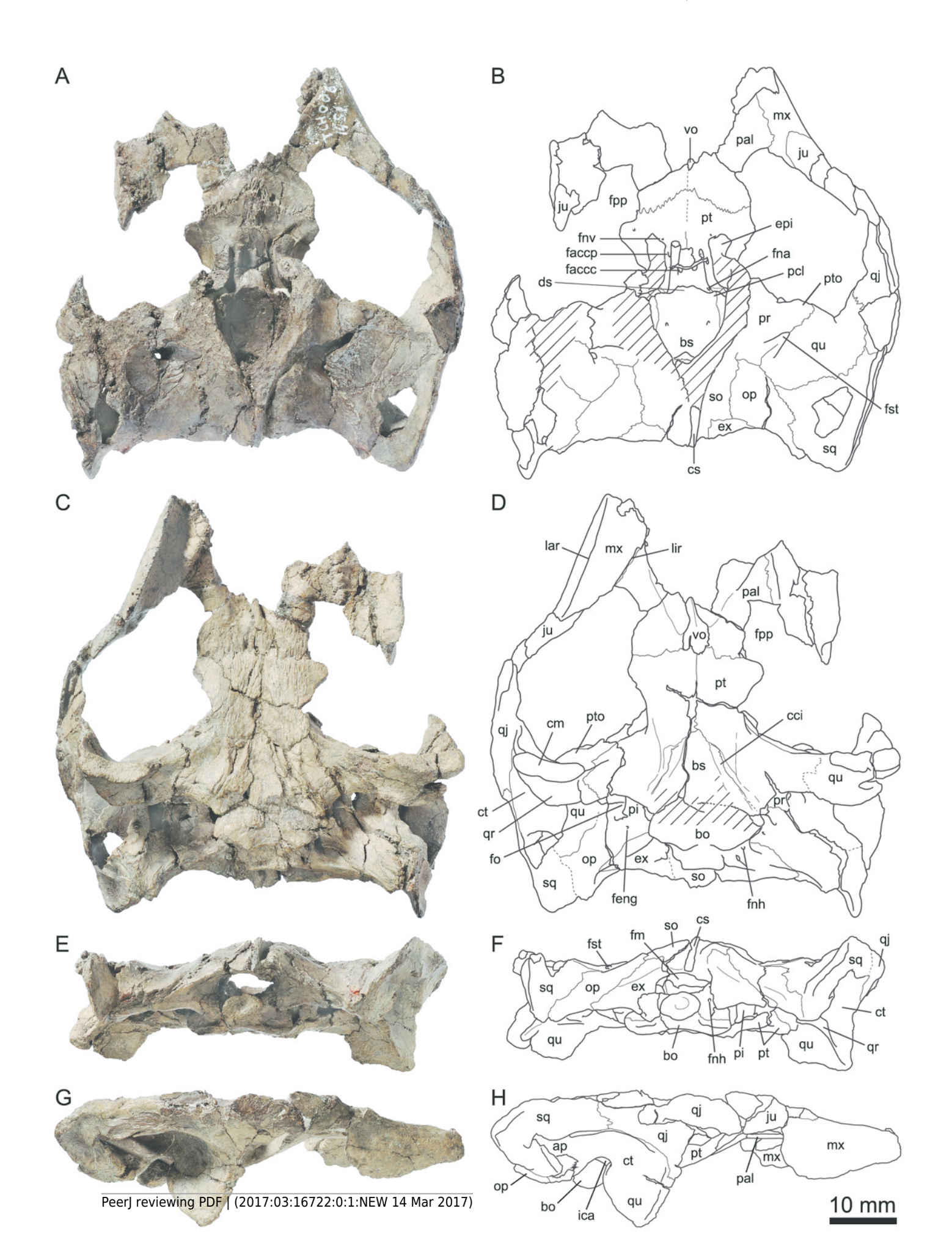
Cranium in dorsal (A, B), ventral (C, D), anterior (E, F), posterior (G, H), right lateral (I, J), and left lateral (K, L) views. Gray areas indicate disarticulated sutural surfaces. Hatchings represent damaged areas. Abbreviations: ap, antrum postoticum; bo, basioccipital; bs, basisphenoid; ccc, canalis caroticus cerebralis; cci, canalis caroticus internus; cs, crista supraoccipitalis; ct, cavum tympani; ds, dorsum sellae; epi, epipterygoid; ex, exoccipital; fce, fossa cartilaginis epipterygoidei; feng, foramen externum nervi glossopharyngei; fna, foramen nervi abducentis; fnh, foramen nervi hypoglossi; fnt, foramen nervi trigemini; fo, fenestra ovalis; fp, fenestra perilymphatica; fst, foramen stapedio-temporale; ica, incisura columellae auris; op, opisthotic; pa, parietal; pi, processus interfenestralis; pcl, processus clinoideus; ppe, processus pterygoideus externus; pr, prootic; pt, pterygoid; ptf, pterygoid fossa; pto, processus trochlearis oticum; qj, quadratojugal; qr, quadrate ridge; qu, quadrate; so, supraoccipital; sq, squamosal; tra, trabecula; un. f., unnamed foramen.





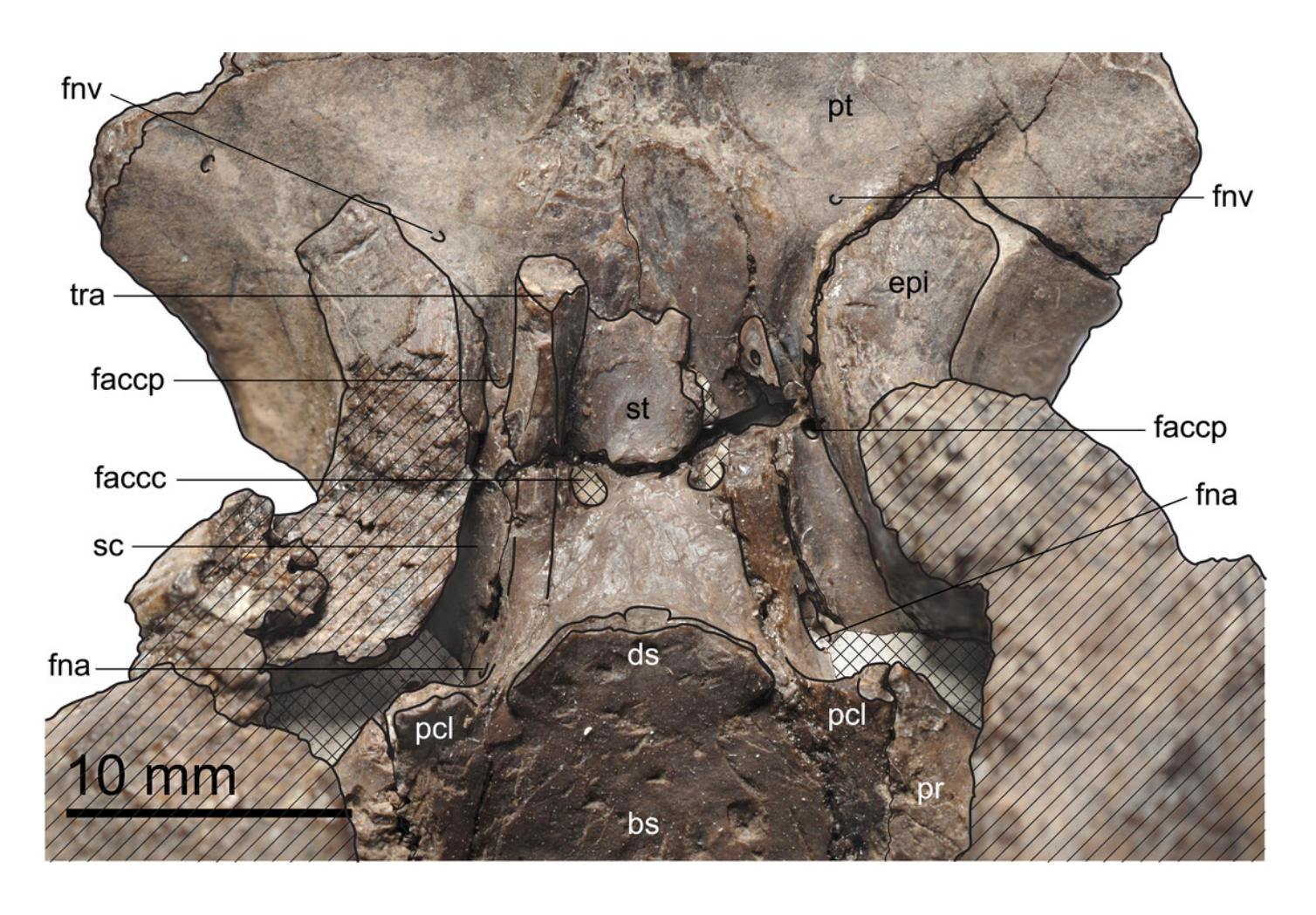
MJSN TCH006-1451, paratype of *Plesiochelys bigleri* (Kimmeridgian, Porrentruy, Switzerland).

Cranium in dorsal (A, B), ventral (C, D), posterior (E, F), and right lateral (G, H) views. Hatchings represent damaged areas. Abbreviations: ap, antrum postoticum; bo, basioccipital; bs, basisphenoid; cci, canalis caroticus internus; cm, condylus mandibularis; cs, crista supraoccipitalis; ct, cavum tympani; ds, dorsum sellae; epi, epipterygoid; ex, exoccipital; faccc, foramen anterius canalis carotici cerebralis; faccp, foramen anterius canalis carotici palatinum; feng, foramen externum nervi glossopharyngei; fm, foramen magnum; fna, foramen nervi abducentis; fnh, foramen nervi hypoglossi; fnv, foramen nervi vidiani; fo, fenestra ovalis; fpp, foramen palatinum posterius; fst, foramen stapedio-temporale; ica, incisura columellae auris; ju, jugal; lar, labial ridge; lir, lingual ridge; mx, maxilla; op, opisthotic; pal, palatine; pi, processus interfenestralis; pcl, processus clinoideus; pr, prootic; pt, pterygoid; pto, processus trochlearis oticum; qj, quadratojugal; qr, quadrate ridge; qu, quadrate; so, supraoccipital; sq, squamosal; vo, vomer.



MJSN TCH006-1451, paratype of *Plesiochelys bigleri* (Kimmeridgian, Porrentruy, Switzerland).

Dorsal view of the dorsum sellae and sella turcica region. Hatchings represent damaged areas. The lattice pattern represents matrix infilling. Abbreviations: bs, basisphenoid; ds, dorsum sellae; epi, epipterygoid; faccc, foramen anterius canalis carotici cerebralis; faccp, foramen anterius canalis carotici palatinum; fna, foramen nervi abducentis; fnv, foramen nervi vidiani; pcl, processus clinoideus; pr, prootic; pt, pterygoid; sc, sulcus cavernosus; st, sella turcica; tra, trabecula.

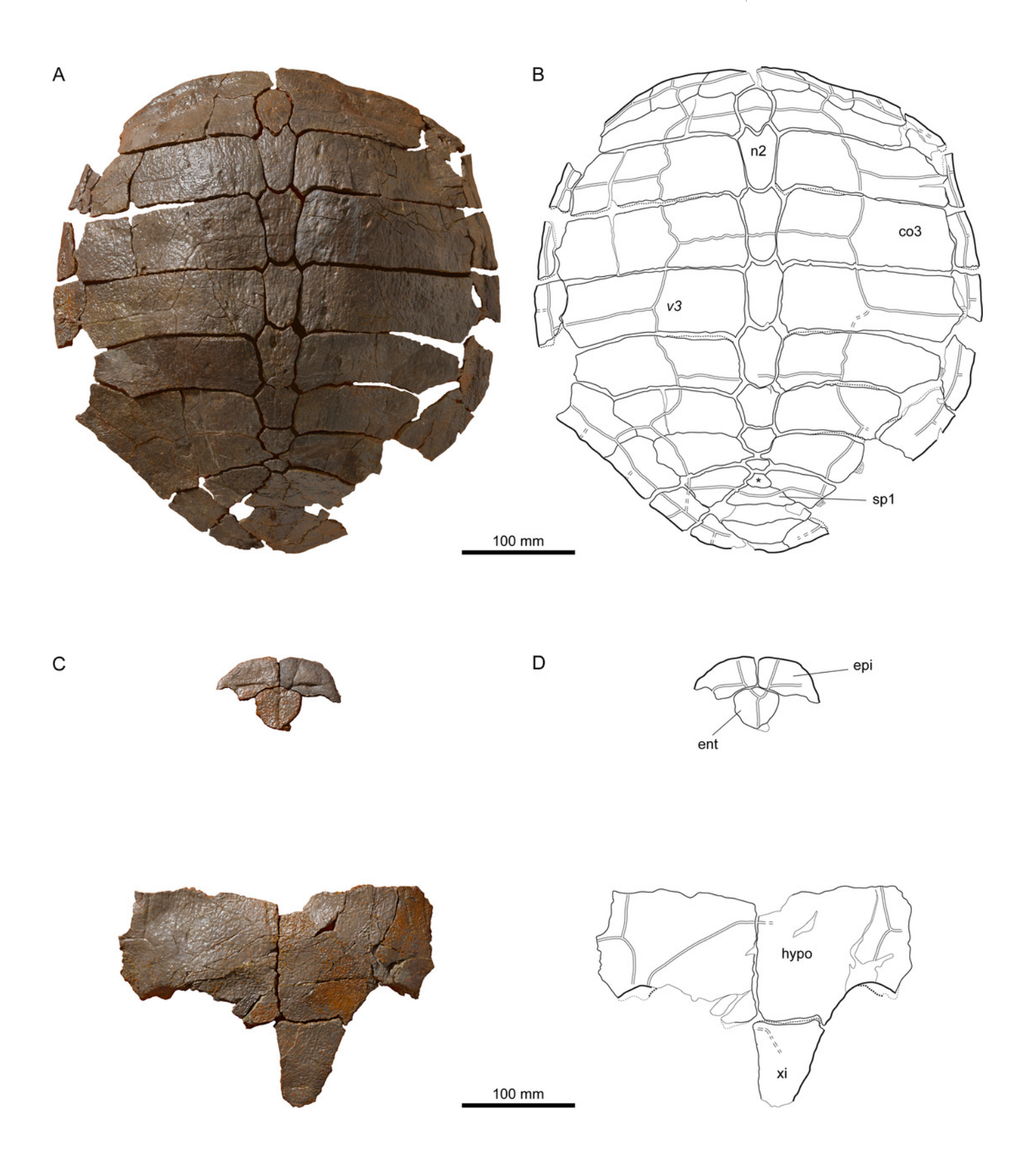




MJSN TCH007-252, holotype of *Plesiochelys bigleri* (Kimmeridgian, Porrentruy, Switzerland).

(A, B) carapace; (C, D) plastron. Line width indicates natural borders (thick lines), bone sutures (medium lines), and fractures (thin lines); double lines indicate scale sulci.

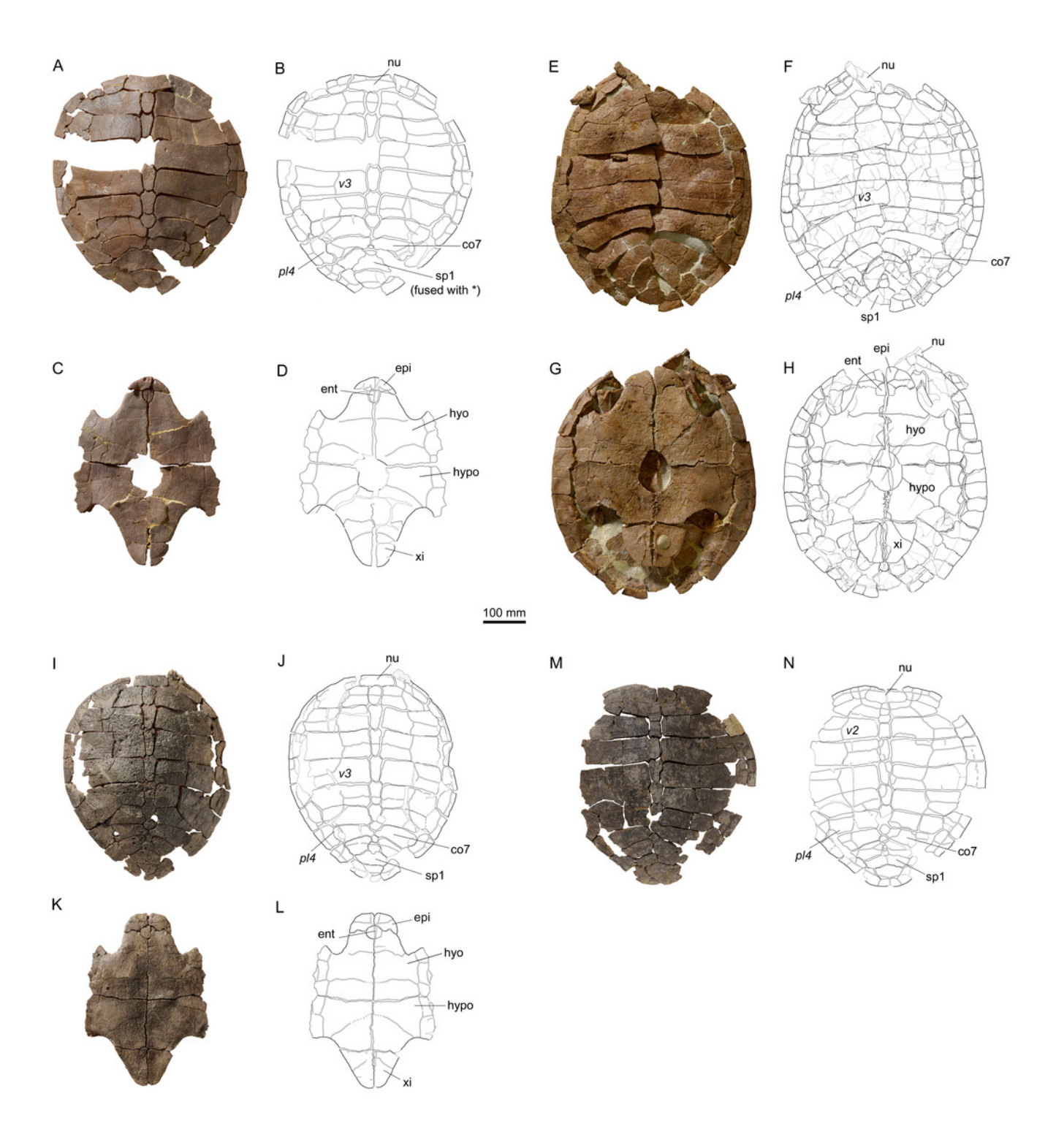
Abbreviations: co, costal; ent, entoplastron; epi, epiplastron; hypo, hypoplastron; n, neural; sp, supragygal; v, vertebral scale; xi, xiphiplastron; \*, intermediate element (see text).





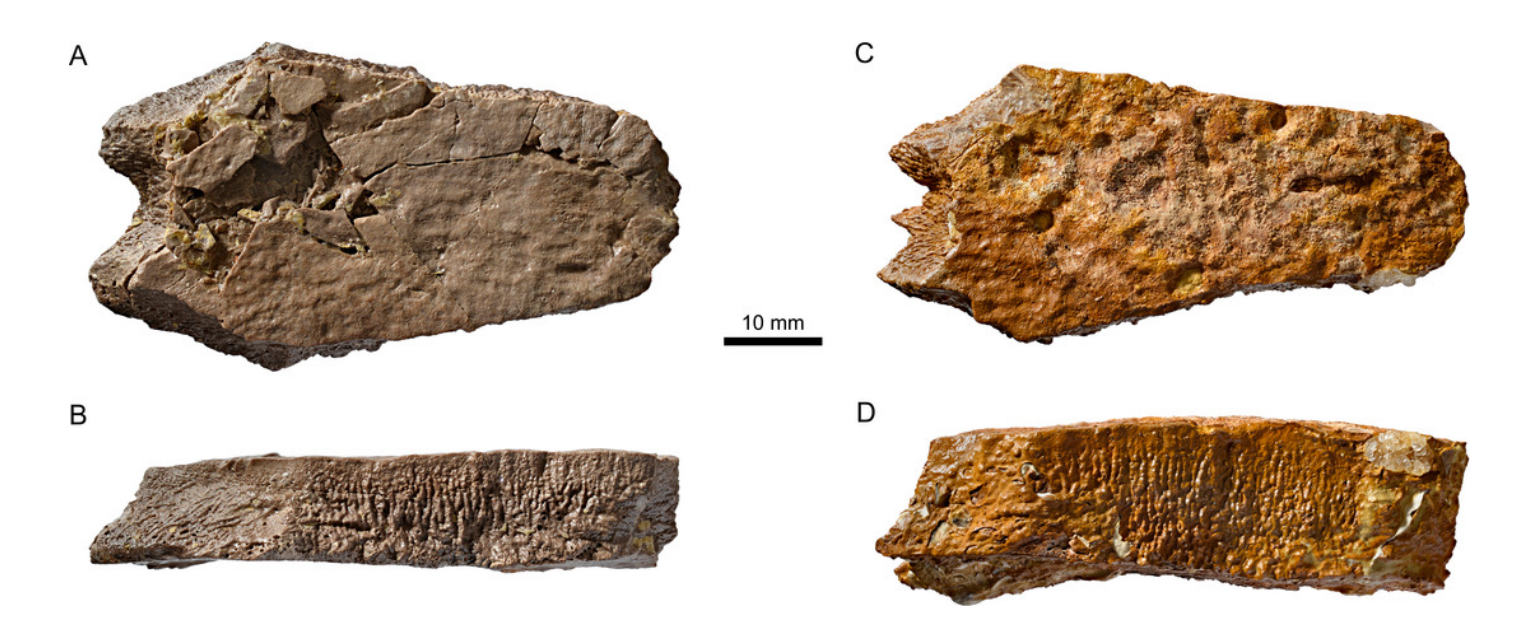
Shells of Plesiochelys bigleri.

Carapace (A, B) and plastron (C, D) of specimen MJSN TCH006-1420 (Kimmeridgian, Porrentruy, Switzerland); carapace (E, F) and plastron (G, H) of specimen MJSN BSY006-307 (Kimmeridgian, Porrentruy, Switzerland); carapace (I, J) and plastron (K, L) of specimen MJSN SCR011-140 (Kimmeridgian, Porrentruy, Switzerland); carapace (M, N) of specimen MJSN TCH005-42 (Kimmeridgian, Porrentruy, Switzerland). Line width indicates natural borders (thick lines), bone sutures (medium lines), and fractures (thin lines); double lines indicate scale sulci. Abbreviations: co, costal; ent, entoplastron; epi, epiplastron; hyo, hyoplastron; hypo, hypoplastron; nu, nuchal; pl, pleural scale; sp, supragygal; v, vertebral scale; xi, xiphiplastron; \*, intermediate element (see text).



Neural bones of *Plesiochelys bigleri* and *Plesiochelys etalloni* (Kimmeridgian, Porrentruy, Switzerland).

Neural 4 of specimen MJSN TCH006-1420 (*Plesiochelys bigleri*) in dorsal (A) and lateral left view (B); neural 4 of specimen MJSN BSY006-347 (*Plesiochelys etalloni*) in dorsal (C) and lateral left view (D).



MJSN TCH005-42, Plesiochelys bigleri (Kimmeridgian, Porrentruy, Switzerland).

Left scapula in lateral (A) and medial view (B).



MJSN TCH007-252, holotype of *Plesiochelys bigleri* (Kimmeridgian, Porrentruy, Switzerland).

Right humerus in dorsal (A), anterior (B), ventral (C), and posterior view (D); left humerus in dorsal (E), anterior (F), ventral (G), and posterior view (H).





MJSN TCH007-252, holotype of *Plesiochelys bigleri* (Kimmeridgian, Porrentruy, Switzerland).

Right radius in dorsal (A), medial (B), ventral (C), and lateral view (D); right ulna in dorsal (E), medial (F), ventral (G), and lateral view (H).





MJSN BSY006-307, Plesiochelys bigleri (Kimmeridgian, Porrentruy, Switzerland).

Pelvis in right lateral view.





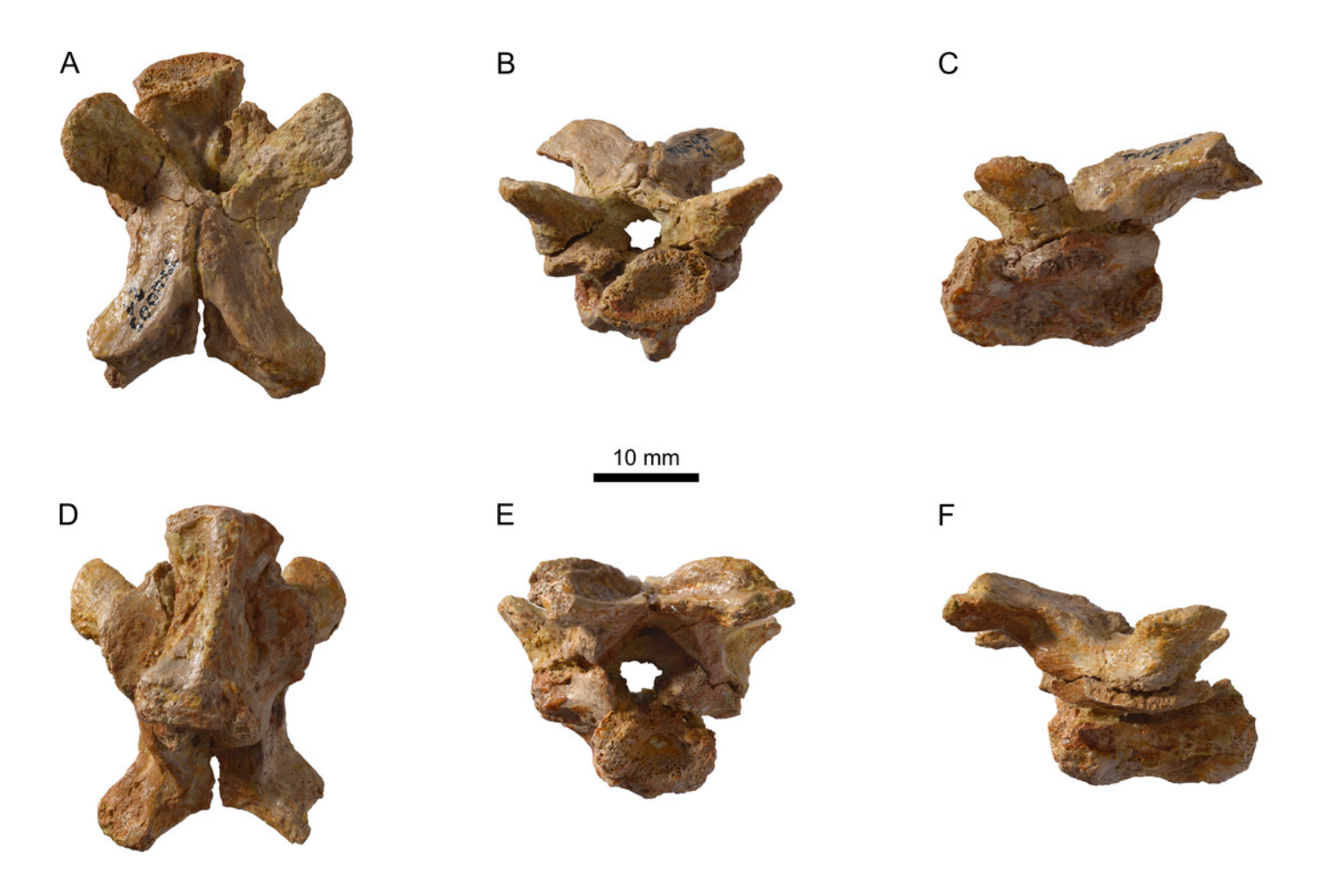
MJSN SCR010-1279, Plesiochelys bigleri (Kimmeridgian, Porrentruy, Switzerland).

Right femur in dorsal (A), anterior (B), ventral (C), and posterior view (D); left fibula in dorsal (E), medial (F), ventral (G), and lateral view (H).



MJSN TCH005-21, Plesiochelys bigleri (Kimmeridgian, Porrentruy, Switzerland).

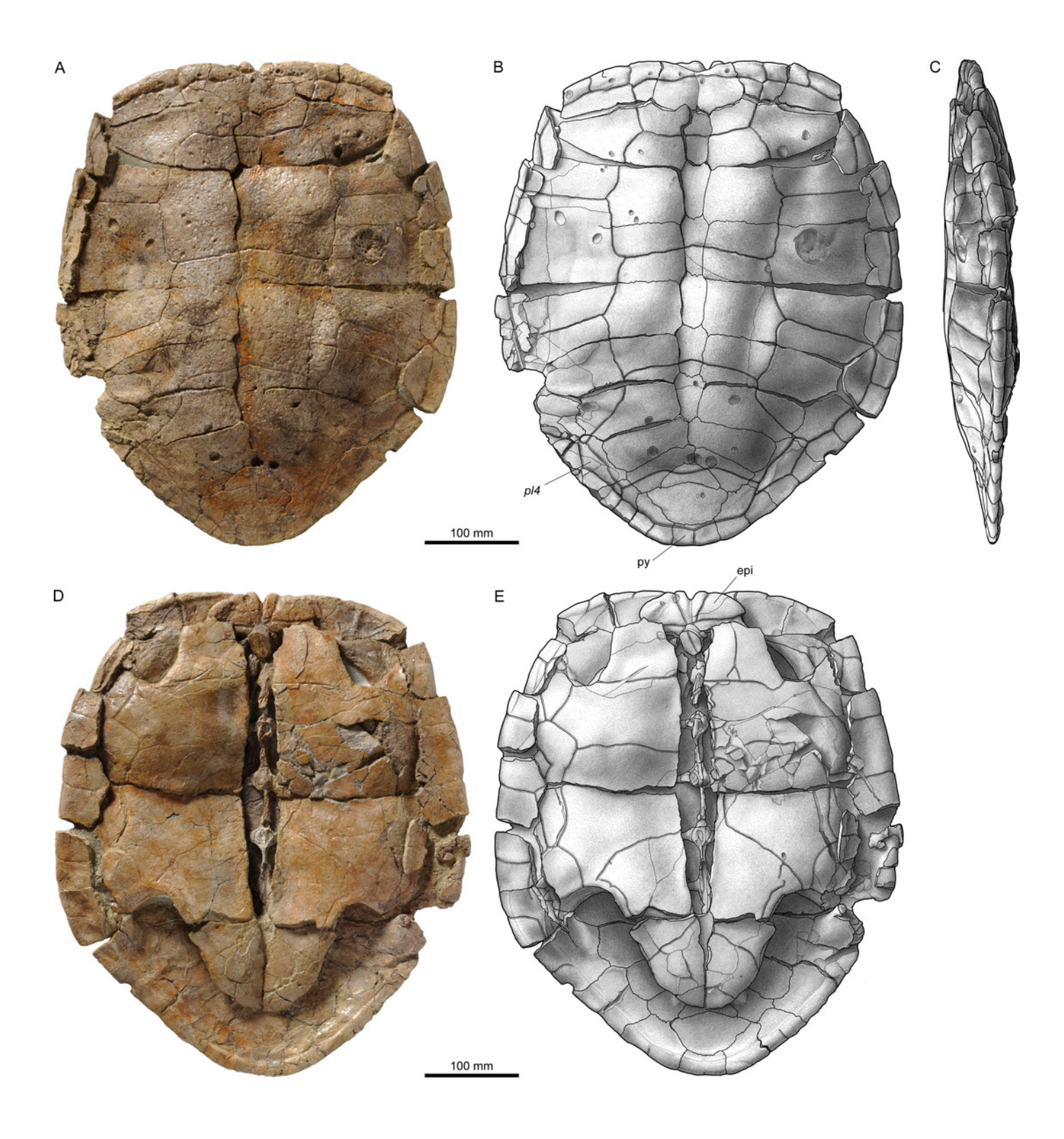
Cervical vertebra in dorsal (A), anterior (B), left lateral (C), ventral (D), posterior (E), and right lateral view (F).





MJSN TCH006-574, Plesiochelys etalloni (Kimmeridgian, Porrentruy, Switzerland).

Carapace in dorsal (A, B) and right lateral view (C); plastron in ventral view (D, E). Line width indicates natural borders (thick lines), bone sutures (medium lines), and fractures (thin lines); double lines indicate scale sulci. Abbreviations: epi, epiplastron; pl, pleural scale; py, pygal.





Neural bone thickness in *Plesiochelys etalloni* and *Plesiochelys bigleri*.

Statistical analysis of mean neural length, mean neural thickness, and corresponding length/thickness ratio (see text) for 25 specimens of *Plesiochelys bigleri* (green), 8 specimens of *Plesiochelys etalloni* (blue), and 10 indeterminate specimens (*Plesiochelys* sp.; gray). (A) Mean length/thickness scatter-plot (specimen numbers are indicated for indeterminate specimens). (B) Length and thickness measurements on the fifth neural bone of specimen BSY006-307 (scale bar = 20mm). (C) Discriminant histogram. (D-F) Box-and-whisker plots for mean length, mean thickness, and length/thickness ratio, respectively.

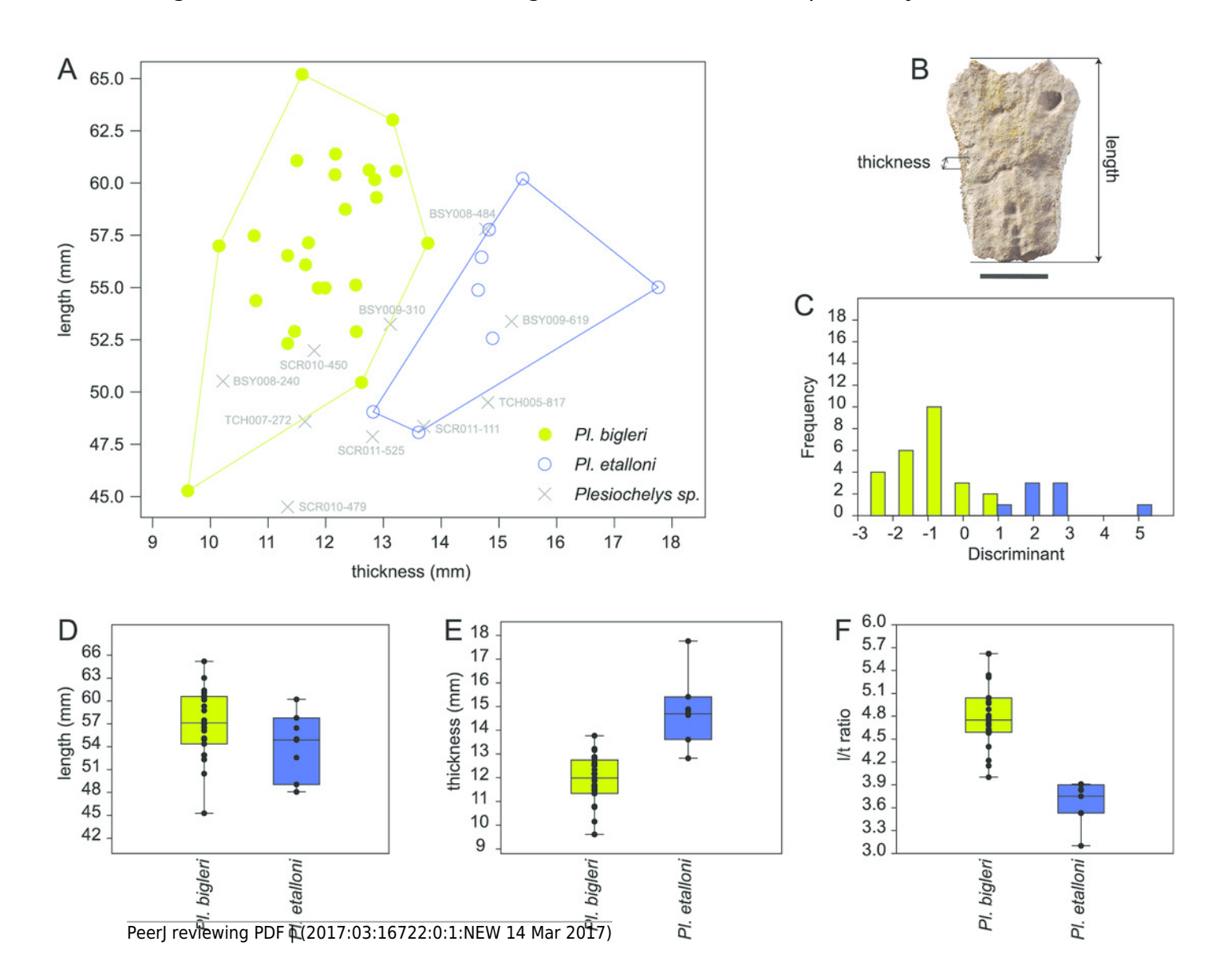




#### Table 1(on next page)

The new *Plesiochelys* material from Porrentruy.

42 specimens are attributed to the new species *Plesiochelys bigleri*, 15 specimens to *Plesiochelys etalloni*, and 24 specimens to *Plesiochelys* sp.



| Plesiochelys bigleri |                  | Plesiochelys etalloni | Plesiochelys sp. |
|----------------------|------------------|-----------------------|------------------|
| MJSN BSY006-307      | MJSN SCR011-37   | MJSN BSY006-347       | MJSN BSY003-1    |
| MJSN BSY006-326      | MJSN SCR011-140  | MJSN BSY006-376       | MJSN BSY008-240  |
| MJSN BSY007-147      | MJSN SCR011-148  | MJSN BSY007-205       | MJSN BSY008-484  |
| MJSN BSY007-257      | MJSN SCR011-160  | MJSN BSY009-694       | MJSN BSY008-674  |
| MJSN BSY008-206      | MJSN SCR011-276  | MJSN SCR003-1011      | MJSN BSY009-171  |
| MJSN BSY008-242      | MJSN SCR011-413  | MJSN SCR008-33        | MJSN BSY009-310  |
| MJSN BSY008-512      | MJSN TCH005-16   | MJSN SCR010-382       | MJSN BSY009-619  |
| MJSN BSY008-567      | MJSN TCH005-21   | MJSN SCR011-415       | MJSN SCR010-413  |
| MJSN BSY008-848      | MJSN TCH005-42   | MJSN TCH005-216       | MJSN SCR010-450  |
| MJSN BSY009-639      | MJSN TCH005-464  | MJSN TCH005-332       | MJSN SCR010-479  |
| MJSN BSY009-743      | MJSN TCH005-819  | MJSN TCH005-457       | MJSN SCR010-559  |
| MJSN BSY009-815      | MJSN TCH006-145  | MJSN TCH006-574       | MJSN SCR010-560  |
| MJSN BSY009-892      | MJSN TCH006-767  | MJSN TCH007-265       | MJSN SCR010-561  |
| MJSN CRT007-2        | MJSN TCH006-1420 | MJSN TCH007-505       | MJSN SCR010-562  |
| MJSN SCR010-327      | MJSN TCH006-1451 | MJSN TCH007-771       | MJSN SCR011-111  |
| MJSN SCR010-342      | MJSN TCH007-252  |                       | MJSN SCR011-525  |
| MJSN SCR010-1009     | MJSN TCH007-371  |                       | MJSN TCH005-286  |
| MJSN SCR010-1047     | MJSN TCH007-516  |                       | MJSN TCH005-817  |
| MJSN SCR010-1196     | MJSN TCH007-519  |                       | MJSN TCH006-776  |
| MJSN SCR010-1279     | MJSN VTT006-299  |                       | MJSN TCH006-787  |
| MJSN SCR011-30       | MJSN VTT006-579  |                       | MJSN TCH007-62   |
|                      |                  |                       | MJSN TCH007-272  |
|                      |                  |                       | MJSN TCH007-541  |
|                      |                  |                       | MJSN TCH007-580  |



#### Table 2(on next page)

Length and width measurements of the skull in *Plesiochelys bigleri*.

These measurements should be compared with those of other plesiochelyid skulls (Anquetin, Püntener & Billon-Bruyat, 2015: table 1).



|             | Total length from       | Length from pt-vo/pal | Width at the level of |  |
|-------------|-------------------------|-----------------------|-----------------------|--|
|             | condylus occipitalis to | suture to condylus    | the condyli           |  |
| Specimen    | tip of the snout (mm)   | occipitalis (mm)      | mandibularis (mm)     |  |
| TCH007-252  | -                       | $38.5^{a}$            | 60.6                  |  |
| TCH006-1451 | $59.8^{a}$              | 34.4                  | 60.0                  |  |

1 2

<sup>&</sup>lt;sup>a</sup> Specimen incomplete



#### Table 3(on next page)

Measurements used for the analysis of neural thickness in *Plesiochelys* spp.

Mean neural length, mean neural thickness, and mean length/mean thickness ratio measured for selected specimens referred to *Plesiochelys bigleri*, *Plesiochelys etalloni*, and *Plesiochelys* sp. Measurements are expressed in millimeters. See Table S1 for original measurements. All specimens are housed at the MJSN.



| Specimen    | Identification | Mean length | Mean thickness | Ratio |
|-------------|----------------|-------------|----------------|-------|
| BSY006-307  | Pl. bigleri    | 60.62       | 12.75          | 4.75  |
| TCH007-252  | Pl. bigleri    | 56.99       | 10.15          | 5.62  |
| SCR011-140  | Pl. bigleri    | 57.48       | 10.76          | 5.34  |
| BSY009-815  | Pl. bigleri    | 57.12       | 13.77          | 4.15  |
| BSY007-257  | Pl. bigleri    | 45.27       | 9.61           | 4.71  |
| SCR011-148  | Pl. bigleri    | 52.89       | 12.53          | 4.22  |
| SCR011-413  | Pl. bigleri    | 54.98       | 11.99          | 4.59  |
| TCH006-1420 | Pl. bigleri    | 56.09       | 11.65          | 4.81  |
| SCR011-276  | Pl. bigleri    | 60.57       | 13.22          | 4.58  |
| VTT006-299  | Pl. bigleri    | 61.39       | 12.17          | 5.04  |
| TCH005-16   | Pl. bigleri    | 61.07       | 11.50          | 5.31  |
| TCH005-464  | Pl. bigleri    | 57.14       | 11.70          | 4.89  |
| TCH005-21   | Pl. bigleri    | 63.02       | 13.16          | 4.79  |
| SCR011-37   | Pl. bigleri    | 52.90       | 11.46          | 4.61  |
| BSY008-206  | Pl. bigleri    | 59.31       | 12.88          | 4.60  |
| SCR010-1279 | Pl. bigleri    | 65.20       | 11.59          | 5.62  |
| VTT006-579  | Pl. bigleri    | 54.98       | 11.87          | 4.63  |
| TCH006-145  | Pl. bigleri    | 52.32       | 11.34          | 4.61  |
| BSY009-892  | Pl. bigleri    | 60.16       | 12.85          | 4.68  |
| TCH005-819  | Pl. bigleri    | 60.40       | 12.16          | 4.97  |
| BSY006-326  | Pl. bigleri    | 54.37       | 10.79          | 5.04  |
| SCR010-1009 | Pl. bigleri    | 56.53       | 11.34          | 4.99  |
| SCR011-160  | Pl. bigleri    | 58.74       | 12.34          | 4.76  |
| SCR010-1196 | Pl. bigleri    | 55.12       | 12.52          | 4.40  |
| TCH006-767  | Pl. bigleri    | 50.46       | 12.62          | 4.00  |
| BSY009-694  | Pl. etalloni   | 57.77       | 14.83          | 3.90  |
| SCR011-415  | Pl. etalloni   | 48.07       | 13.61          | 3.53  |
| BSY006-347  | Pl. etalloni   | 56.45       | 14.70          | 3.84  |
| BSY007-205  | Pl. etalloni   | 60.21       | 15.41          | 3.91  |
| SCR008-33   | Pl. etalloni   | 55.01       | 17.76          | 3.10  |
| SCR010-382  | Pl. etalloni   | 49.05       | 12.82          | 3.83  |



#### **PeerJ**

| TCH007-265 | Pl. etalloni     | 52.57 | 14.89 | 3.53 |
|------------|------------------|-------|-------|------|
| TCH007-505 | Pl. etalloni     | 54.88 | 14.64 | 3.75 |
| BSY009-310 | Plesiochelys sp. | 53.24 | 13.12 | 4.06 |
| TCH007-272 | Plesiochelys sp. | 48.59 | 11.64 | 4.18 |
| TCH005-817 | Plesiochelys sp. | 49.50 | 14.81 | 3.34 |
| SCR010-450 | Plesiochelys sp. | 51.98 | 11.80 | 4.40 |
| SCR010-479 | Plesiochelys sp. | 44.50 | 11.34 | 3.92 |
| SCR011-525 | Plesiochelys sp. | 47.86 | 12.81 | 3.74 |
| BSY009-619 | Plesiochelys sp. | 53.38 | 15.22 | 3.51 |
| BSY008-240 | Plesiochelys sp. | 50.52 | 10.22 | 4.95 |
| SCR011-111 | Plesiochelys sp. | 48.35 | 13.70 | 3.53 |
| BSY008-484 | Plesiochelys sp. | 57.80 | 14.77 | 3.91 |

1



#### Table 4(on next page)

Classification of indeterminate specimens.

Comparison of the tentative classifications of indeterminate specimens (*Plesiochelys* sp.) based on the length/thickness scatter plot (Fig. 17A) and the discriminant analysis (Fig. 17C). All specimens are housed at the MJSN.



#### **PeerJ**

| Specimen   | Scatter plot | Discriminant analysis |
|------------|--------------|-----------------------|
| BSY009-310 | Pl. bigleri  | Pl. etalloni          |
| TCH007-272 | Pl. bigleri  | Pl. bigleri           |
| TCH005-817 | Pl. etalloni | Pl. etalloni          |
| SCR010-450 | Pl. bigleri  | Pl. bigleri           |
| SCR010-479 | ?            | Pl. bigleri           |
| SCR011-525 | Pl. etalloni | Pl. etalloni          |
| BSY009-619 | Pl. etalloni | Pl. etalloni          |
| BSY008-240 | Pl. bigleri  | Pl. bigleri           |
| SCR011-111 | Pl. etalloni | Pl. etalloni          |
| BSY008-484 | Pl. etalloni | Pl. etalloni          |

1